Development and Validation of a Novel Biomechanical Testing Setup and Procedure for Olecranon Fracture Fixation Assessment

by

Saaransh Jain

A Thesis Presented in Partial Fulfillment
of the Requirements for the Degree
Master of Science

Approved November 2015 by the
Graduate Supervisory Committee:

Jeffrey LaBelle, Co-Chair
James Abbas, Co-Chair
Marc Jacofsky

ARIZONA STATE UNIVERSITY

December 2015

ABSTRACT

Olecranon fractures account for approximately 10% of upper extremity fractures and 95% of them require surgical fixation. Most of the clinical, retrospective and biomechanical studies have supported plate fixation over other surgical fixation techniques since plates have demonstrated low incidence of reoperation, high fixation stability and resumption of activities of daily living (ADL) earlier. Thus far, biomechanical studies have been helpful in evaluating and comparing different plate fixation constructs based on fracture stability. However, they have not provided information that can be used to design rehabilitation protocols such as information that relates load at the hand with tendon tension or load at the interface between the plate and the bone. The set-ups used in biomechanical studies have included simple mechanical testing machines that either measured construct stiffness by cyclic loading the specimens or construct strength by performing ramp load until failure. Some biomechanical studies attempted to simulate tendon tension but the *in-vivo* tension applied to the tendon remains unknown. In this study, a novel procedure to test the olecranon fracture fixation using modern olecranon plates was developed to improve the biomechanical understanding of failures and to help determine the weights that can be safely lifted and the range of motion (ROM) that should be performed during rehabilitation procedures.

Design objectives were defined based on surgeon's feedback and analysis of unmet needs in the area of biomechanical testing. Four pilot cadaveric specimens were prepared to run on an upper extremity feedback controller and the set-up was validated based on the design objectives. Cadaveric specimen preparation included a series of steps such as dissection, suturing and potting that were standardized and improved iteratively after pilot testing. Additionally, a fracture and plating protocol was developed and fixture lengths were

standardized based on anthropometric data. Results from the early pilot studies indicated shortcomings in the design, which was then iteratively refined for the subsequent studies. The final pilot study demonstrated that all of the design objectives were met. This system is planned for use in future studies that will assess olecranon fracture fixation and that will investigate the safety of rehabilitation protocols.

ACKNOWLEDGMENTS

First and foremost, I thank my thesis committee Dr. James Abbas, Dr. Jeffery LaBelle and Dr. Marc Jacofsky for offering me an exhaustive graduate school experience by giving me intellectual freedom in my work, letting me engage in new ideas and brainstorming on critical research issues. Additionally, I would like to thank engineers and interns from The MORE Foundation, Aniruddh Nayak, Madusudan Narayanan and Robert Boudreaux for their interest in my work. Every result described in this thesis was accomplished with the help and support of fellow labmates and collaborators. Research Associate, Kellen Worhacz help has been invaluable. He trained me on all the dissection skills exercised in this thesis. Discussions with clinical researcher in the lab, Neil Olmscheid in debugging suturing issues, and his help during experiments was very productive. Finally, I would like to extend my gratitude to my friends, my parents (Dr. Satish Jain and Dr. Bandana Jain), my brother (Chitrank Jain) and my fiancé (Chandni Jain) for their unconditional support all through my graduate research during my Masters at Arizona State University.

TABLE OF CONTENTS

Page

LIST OF TABLES

Table Page

LIST OF FIGURES

Figure Page

Figure Page

Figure Page

Figure Page

CHAPTER 1

INTRODUCTION

1.1 Elbow Joint Anatomy

The elbow joint is a complex synovial hinge joint formed between the humerus in the upper arm and the radius and ulna in the forearm [See Figure 1]. The distal end of the humerus flares out into two rounded protrusions called epicondyles (medial and lateral). The proximal end of the ulna has two protrusions: the olecranon process (bony prominence of elbow tip) and the coronoid process. The notch defined by the olecranon proximally, and the coronoid distally, is the semilunar notch, which articulates with the trochlea of the humerus to form the humero-ulnar joint. These protrusions and corresponding depressions help to keep the segments aligned as the elbow is rotated. The other joint of elbow is the joint between radius and humerus, which is formed by the head of the radius and capitulum of the humerus.

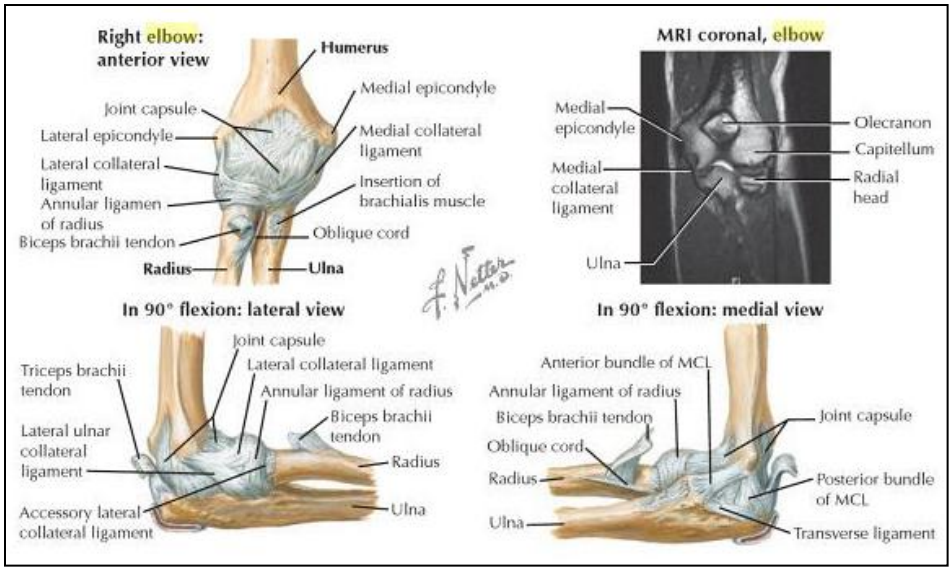

Figure 1: Elbow Joint Anatomy. Netter [25], Page 119

There are several muscles that flex, extend or rotate the forearm that are broadly grouped as the flexor group and the extensor group. The flexor group consists of

the brachialis, biceps brachii, and the brachioradialis. The brachialis, which is the primary flexor of the elbow, originates at the anterio-distal surface of humerus and inserts at coronoid process of ulna. The extensor group consists of the triceps brachii and anconeus. The triceps brachii is a three headed muscle which originates from different regions:

a) Long head: Infraglenoid tubercle of scapula

b) Lateral head: Upper half of posterior humerus

c) Medial head: Lower half posterior humerus inferomedial to spiral groove and both intermuscular septa

All of them insert in the form of one tendon at olecranon process of ulna.

1.1.1 Olecranon Process

The Olecranon is a bony prominence located at the proximal end of the ulna, curves around the distal part of the humerus to encapsulate the elbow joint [See Figure 2]. The posterior side of the olecranon marks a rough impression for the triceps brachii insertion and its anterior surface forms a smooth and concave semilunar notch, which holds the trochlea of the distal humerus.

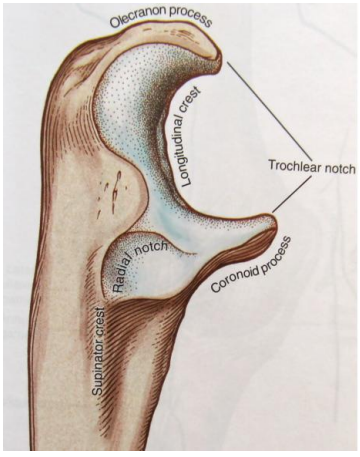

Figure 2: Olecranon Process and Region Around it. Neumann [26], page 177

1.2 Olecranon Fractures

Olecranon fractures (elbow fractures) can occur to people in all age groups: these are typically low-energy injuries in the older population and higher-energy mechanisms in the younger age group. These fractures are relatively common injuries, accounting for approximately 10% of upper extremity fractures in adults [1]. An olecranon fracture can occur in two forms of injuries: 1) Indirect injury, in which a forceful contraction on the triceps muscle pulls the proximal olecranon leading to a transverse or oblique fracture. 2) Direct injury, in which a force is applied directly to the olecranon, leading to a more comminuted fracture pattern.

The actual mechanism of injury often dictates the fracture pattern and the specific management approach. Different classifications are used to define the olecranon fracture in clinical and academic settings. They are as follows:

1) Mayo Classification

This classification is widely used in clinical practice and is based on the stability, the displacement and the comminution of the fracture [See Figure 3].

Type I: Non-displaced fractures – It can be either non-comminuted (Type IA) or comminuted (Type IB).

Type II: Displaced, stable fractures – In this pattern, the proximal fracture fragment is displaced more than 3 mm, but the collateral ligaments are intact, which provides elbow stability. It can be either non-comminuted (Type IIA) or comminuted (Type IIB).

Type III: Displaced instable fracture – In this case, the fracture fragments are displaced and the forearm is instable in relation to the humerus. It is a fracture -dislocation. It also may be either non-comminuted (Type IIIA) or comminuted (Type IIIB).

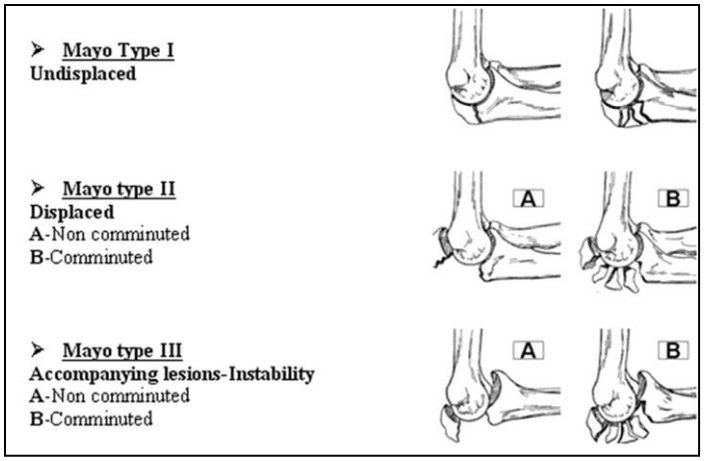

Figure 3: Mayo Classification of Olecranon Fractures [4]

2) AO Classification

This classification incorporates all fractures of the proximal ulna and radius into one group. And this one is subdivided into 3 patterns:

Type A: Extra-articular fractures of the metadiaphysis of either the radius or the ulna.

Type B: Intra-articular fractures of either the radius or ulna

Type C: Complex fractures of both the proximal radius and ulna

There have been multiple attempts to classify the olecranon fractures; some other classifications are Colton, Morrey and Schatzker but the Mayo Classification is most commonly used in clinical practice. Because of subcutaneous location of the olecranon and anatomic particularities involved, most of the fractures (95%) need surgical fixation to allow early range of motion [2, 4].

1.3 Management Approach for Olecranon Fractures

1.3.1 Non-operative Management

Undisplaced olecranon fractures can be treated non-operatively with immobilization of the elbow for few weeks and then gradually returning to exercise.

1.3.2 Open Reduction and Internal Fixation (ORIF)

An open reduction and internal fixation (ORIF) refers to a type of surgery which is used to fix broken bones. In the first part of the surgery, the skin is opened to directly expose the fracture area and the broken bone is reduced (put back into place). In the next part, an internal fixation device such as screws, pins or plates are placed on the bone to secure the fracture site and prevent motion of the bone fragments. There are numerous fracture plates available for the fixation of olecranon fractures and the features of these plates vary between manufacturers and the specific fracture applications.

1.4 Historical Review and Evolution of ORIF Technology

Over many decades of innovation, olecranon fracture fixation has been treated with diverse surgical methods and instruments in order to optimize fixation strength and minimize complications. These diversified variety of constructs include tension band wiring (TBW), plates and screws, staples, sled devices, intramedullary constructs, single screw, and screw plus tension band techniques. Locking plates, intramedullary nails and plates with hooks are some recent development in the area of olecranon fracture fixation. Despite recent advances in ORIF technologies, nonlocked plates, screws, and TBW are still commonly employed [3,4]. TBW is one of the widespread surgical methods for the fixation of olecranon fracture. TBW relies upon the principle of converting posterior tensile forces to articular compressive forces [4]. Although this principle of compression has been classically taught to surgeons in medical community, various studies failed to validate this principle biomechanically [9,10].

Additionally, studies suggest TBW should not be recommended for fractures with displaced and comminuted nature [19]. Although the technique requires minimum soft tissue dissection and periosteal stripping [20], malunion, nonunion, implant prominence and high

hardware removal rate (as high as 100%) are some frequent problems associated with post TBW fixation. [2,3,8,13]. With these traditional fixation methods, patients have had significant restrictions on joint motion for 2 weeks or more and are cautioned against lifting heavy objects for several weeks or even months. In order to reduce and avoid these complications, researchers and clinicians looked for other alternative fixations methods. Over the last two decades, many biomechanical, retrospective and clinical studies have suggested that plate fixation of displaced olecranon fractures gives better results than TBW [5,19].

Hume et al. performed one of the first clinical comparisons of TBW and plate fixation techniques in 41 patients with displaced olecranon fracture. They observed symptomatic metal prominence in the patients post TBW that led him to look for alternative methods such as plate fixation. He published his comparative study based on the scores of pain, range of motion (ROM) and complications after a follow-up period of 28.5 weeks. The data suggested one-third tubular plate fixation results in more anatomic reduction than TBW both clinically and radiographically [19].

Almost after a decade, Bailey et al. conducted a retrospective study to evaluate the functional outcome of the plate fixation for Mayo Type II as well as Type III olecranon fractures. After an average follow up time of 34 months for 25 patients, the outcome displayed high patient satisfaction (9.7/10), low pain rating (1/10), excellent Mayo Elbow performance Index (MEPI) and consistently normal Disability of Arm Shoulder Hand questionnaire (DASH) score [12]. Since then, several clinical and retrospective studies were conducted on modern olecranon plates. Clinical outcomes of the Mayo elbow congruent olecranon plate system (Acumed) was evaluated in 2007 by Anderson et al.[3] and the MEPS, DASH scores were published with results comparable with the results of the Bailey

et al. clinical study. A similar study was carried out by a group of surgeons in 2014 on 2.4mm and 2.7mm plating techniques [13].

One of the earliest biomechanical studies of plate fixation of olecranon fractures was performed by King et al in 1996 [5]. This group used a material testing machine to pull equal load on triceps and brachialis with the elbow placed in different fixed positions of flexion. The focus of this study was to compare lateral and posterior plate locations using a contoured 3.5mm pelvic reconstruction plate, not a plate specifically designed for elbow fractures.

While this study attempted to recreate muscle and joint reaction forces, the authors state that their suture attachment at triceps tendon generally failed between 300-500 N which represents only 7 N (1.6 lbs) of force at the wrist. The authors also stressed that the amount of tension needed in these tendons to move the arm is unknown, even for unloaded active motion early in the rehabilitation process. This study did not address locking plate technology and placed unrealistically low loads across the fracture site due to poor tendon fixation. Prayson et al. [6] tested multiple tension banding and combination wiring techniques for olecranon fractures in cadaver specimens under load, but did not include any plate constructs. One of the drawbacks of this study was that it placed a simulated load on only the triceps tendon. The load was created by holding the tendon rigidly in place while flexing the elbow with the load frame piston.

During a decade-long development in the orthopedic industry, engineers and clinicians realized the advantages of plate fixation of olecranon fractures over TBW. The orthopedic market went through a series of innovations in the area of plates for ORIF. One major advancement was the introduction of locking screws and plate systems. Several new olecranon plate were designed and multiple orthopedic companies like Stryker, Smith and

Nephew, Zimmer, Depuy Synthes, Medartis, Acumed launched different sets of olecranon plates based on the fracture pattern and severity.

It was necessary to evaluate the effectiveness of these new plates, so that the medical community could understand the advantages of plate constructs in olecranon fractures. Therefore, a series of biomechanical tests were performed after the introduction of these modern olecranon plates to evaluate their performance and benefits over conventional techniques. In one study, performed by Buijze et al., the strength and stiffness of locking compression plates (LCP) to one-third tubular plate (TUB) fixation were compared [7]. The stiffness was measured by cyclic loading the specimen and measuring gap at the osteotomy site, where as strength was measured through load to failure.

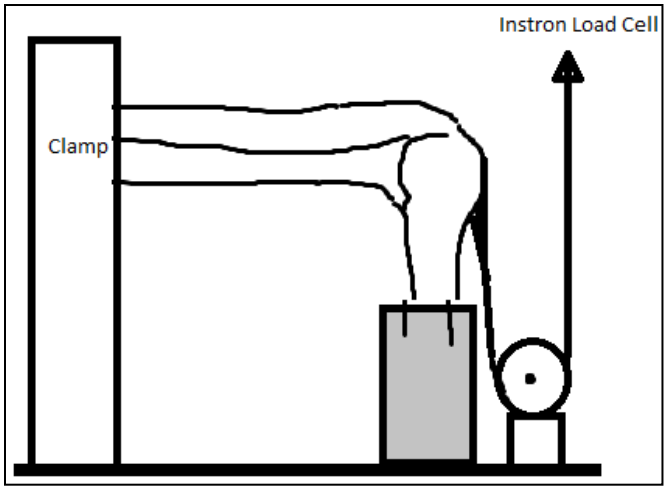

Figure 4: Example of a Set-up where Triceps Tendon Pulled through Instron Machine while Both Ulna and Humerus are Potted [9]

They fixed the failure criteria as the moment required to create a gap of 2 mm at the fracture site or destructive failure. They also recommended that the LCP was a more beneficial fixation device than TUB (conventional plating) because of more axial & angular stability, better rigidity as its proximity with the fracture site and no toggling of unlocked screws. Like Prayson et al., this study also placed a simulated load on only triceps tendon and

flexed the elbow with the load frame piston. Meanwhile in the US, some surgeons were testing a new fixation technique called OlecraNail (a multidirectional locking nail) developed by Mylad Orthopedic Solutions, VA [8].

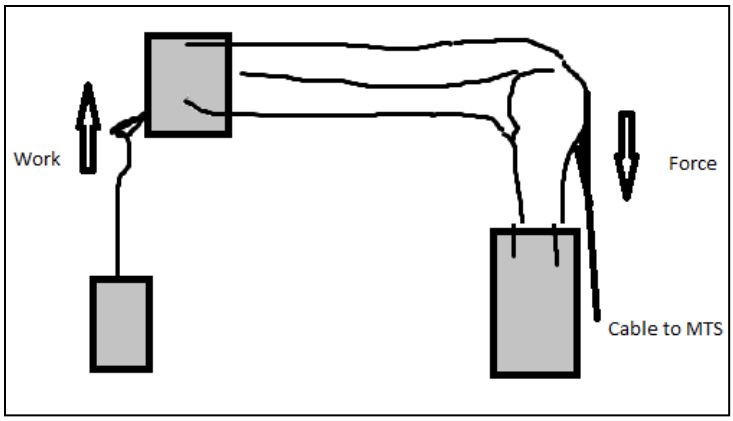

Figure 5: Triceps Tendon Sutured with Nylon Strap and Pulled Through Material Testing Machine, Putting Weight by Hanging on a Hook [8]

Though this biomechanical study was similar to that of [7], they added simulated weights at the end of the ulna/radius based on the activities such as simple active motion and pushing up from a chair. The author set the criteria for failure as fragment displacement of 3mm and increased the weights at the ulna until failure was achieved. As in all other studies, they also used only triceps tendon and pulled it through a uni-axial loading machine [See Figure 5].

In order to address the problem of metal prominence due to poor contour, there has been a drastic change in the design of olecranon plates in last few years. One of the latest innovations in modern locking olecranon plates is the use of proximal tabs or tines. This change in design is aimed to engage the triceps tendon and cortical bone to enhance fixation and increase the congruency. Two such devices are the Smith and Nephew PERI-LOC Olecranon Plate and Depuy Synthes Locking compression plate (LCP) hook plate 3.5.

In 2013, Chen et al. conducted a retrospective study of patients operated with olecranon hook plates called central tension plates (Certificate No. 649355, Patent No. ZL 2008 1 0079748.X) with average follow up of 42 months [17]. They evaluated the quality of reduction through postsurgical radiographical assessment and evaluated recovery through MEP and DASH scores. With high mean MEP scores (93.6), high mean DASH scores and no symptomatic plate removal, the authors concluded that good results can be achieved with these innovative design of plates. But based on a retrospective study it is hard to assess if their contouring with the bone is the reason behind good results. Hence, a biomechanical study should be performed in order to evaluate the congruency better.

1.5 Need Assessment and Objective

In the fixation of olecranon fractures, whether comminuted or simple, most of the biomechanical studies have been helpful in indicating the superiority of plates over other fixation techniques like TBW [2,3,5,8,19]. Other studies have compared plate fixation methods to each other in which they compared the displacement value across the fracture site. However, in the early rehabilitation protocol that can be followed, the amount of weight that can be safely lifted when returning to activities of daily living (ADLs) and the particular range of motion that is safe during rehabilitation remain under-investigated. The shortcomings of the earlier biomechanical testing set-up, especially those attempting to simulate tendon tension, are that the *in vivo* tension applied to the tendon remains unknown [5,8,9,15]. Further, the most comprehensive of these tests were performed with the elbow in static positions, not over a dynamic range of motion [5,8]. **The objective of the current study is to develop a novel procedure to test the olecranon fracture fixation and validate the testing set-up for future biomechanical olecranon fixation studies.** The current study aims to utilize an upper extremity feedback controller to simulate complete

neuromuscular control. This controller allows the elbow to be moved through a dynamic range of motion with and without additional weight in the hand to simulate activities of daily living (ADLs).

1.6 Upper Extremity Feedback Controller

The Musculoskeletal Orthopedic Research and Education Foundation (The MORE Foundation) has developed an in-house a system that can simulate neuromuscular control of the joint using position feedback from the limb to drive tendon displacement. It was initially designed to simulate position control characteristics of in vivo neuromuscular control of the shoulder [20,21]. It is similar to the shoulder controller used by Hansen et. al [11], but it was upgraded and it provides a greater refresh rate for the control loop and an optical position tracking rather than magnetic system, which can be subject to interference from metal objects in the test space.

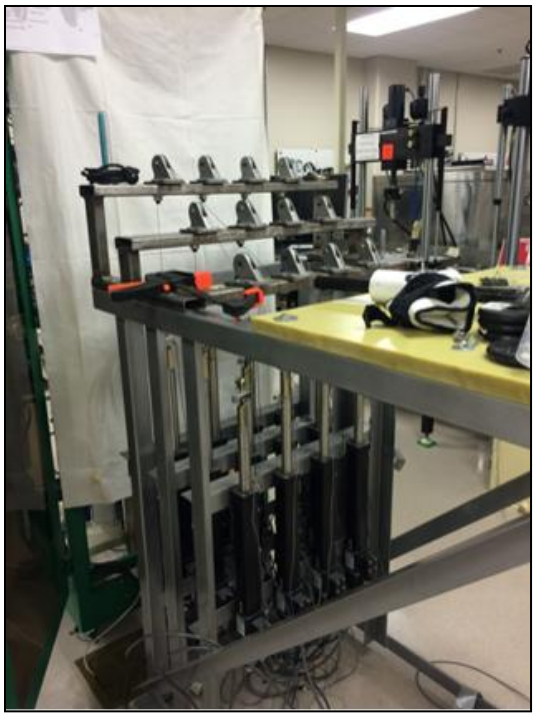

Figure 6: 12 Actuator Set-Up of Upper Extremity Feedback Controller

The device has 12 independent stepper motors that actuate cables that are attached to the bone through sutured tendon. These cables are passed through eyelets or pulleys (positioned at the center of the muscle origin) to approximate the line of action of the muscles and then connected with the right actuator of the controller. The simulator can report the amount of tension required by each muscle to move the bone/joint to the desired position, regardless of how much additional mass is added to the system to simulate functional loads. The motors are always in velocity control within the software. We can use force control or joint position control to create a velocity command. So unless the muscle is in force control, such as brachialis, the force is a reported outcome and not a control input.

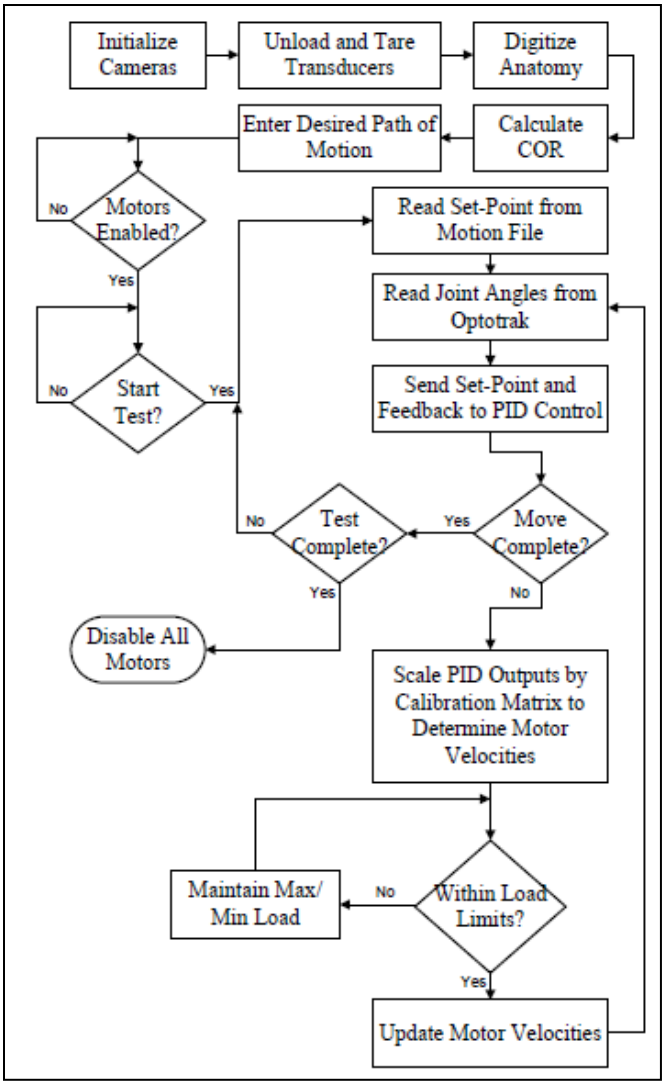

Figure 7: Flow Chart Explaining the Working Process of the Upper Extremity Feedback Controller [Andrew Jaczynski MS thesis (24)]

Therefore, the system reports or records the force value required to generate a given joint position, but it does not technically determine the force. Although this system has worked well for the shoulder studies, it needs to be evaluated and modified for the future elbow fracture studies based on range of motion, number of cycles, weight limits, actuator controls (force or elevation) etc.

In the upper extremity controller, the motors are always in velocity control within the software. In order to create a velocity command, the system can use force control or

joint position control or elevation control. Figure 7 describes the flow diagram of the control strategy of the upper extremity feedback controller. In the case of elbow study, the system can use elevation control for triceps and brachialis and hence the force is a reported outcome. Therefore, the system records the force value required to move the elbow from one angle to another.

CHAPTER 2

SUMMARY OF STUDY DESIGN

The purpose of the study was to develop a novel procedure and platform to perform biomechanical testing of olecranon fracture fixation. The validation of the testing set-up performed in this study can be used to evaluate a variety of elbow fracture types and fixation systems. The first study to be performed after validation will test the performance of olecranon plates [See Figure 8] with tines and without tines to fix a Mayo type IIA olecranon fractures to isolate the effect of tines on fracture stability under simulated activities of daily living.

Four cadaveric arms were dissected, sutured and potted to validate and streamline a novel procedure for testing olecranon fracture fixation with modern olecranon plates. In order to validate the testing procedure and set-up, a layout of all the requirements [see Appendix B] for the successful validation of the testing system, fixtures and procedure was created. Based on these requirements, design objectives were set so that all these requirements could be met in the pilot specimens. The challenges and issues faced were fixed and changes were implemented in the successive pilot testing until an aggressive testing checklist was developed.

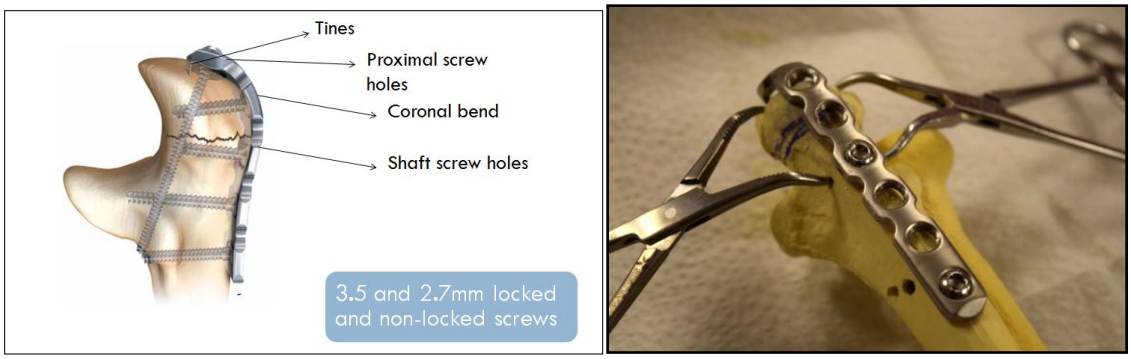

Figure 8: Peri-Loc™ Olecranon Plates of Smith And Nephew [23] Fixed on a Saw Bone Model (First Image, Retrieved from www.ortovit.eu)

First, fresh frozen cadaveric elbows were dissected including removal of all the soft tissues except triceps, brachialis, elbow capsule and radio-ulnar interosseous membrane. After the dissection the elbows was resected to a defined length and potted through **Bondo®** before attaching it onto the upper extremity feedback controller.

A fracture creation and plate fixation protocol was developed using saw bone model [See Appendix A, Page 61]. A standardized Mayo Type IIA transverse fracture in a lateral view was created bilaterally with the help of C-arm fluoroscope [See Figure 9]. Plates received hybrid fixation in the diaphyseal (shaft) holes using unlocked screws in the first and last positions distal to the fracture only. Plate fixation of this fracture type would rarely fail at the diaphysis and locked screws are not necessary at all in these locations (See plating procedure- Appendix A, Page 64). In order to adequately control this study, it was important to have rigid stability between the plate and diaphysis so that motions are focused on the olecranon fragment, where screw cutout was most likely. This is achieved through unlocked screws generating friction of the plate to the bone.

Figure 9: C-arm Flouroscope. Retrieved from http://www.amberusa.com/

The already potted humeral shaft was then fixed in the feedback controller in a particular arrangement which is shown in the Figure 10. The arrangement considered here is

a worst-case scenario, so that the triceps has to maintain maximum load to move the arm from flexion to extension.

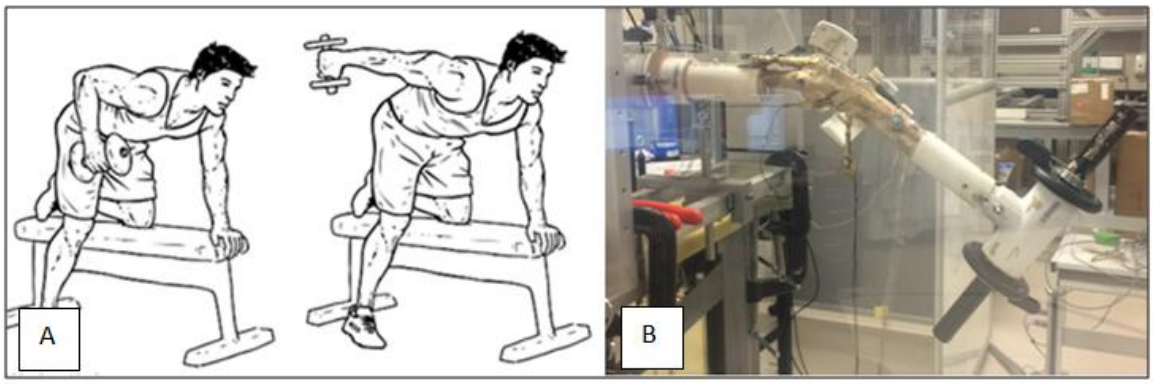

Figure 10 A. Image Shows a Man Performing Triceps Kick Backs in which the Arm is at Parasagittal Plane to the Body while Holding Dumbbells, [Retrieved from http://workoutlabs.com/] B. Set-up Used in the Current Study

The cadaveric elbow was then tested in a neuromuscular simulator that produces realistic muscle forces through a custom closed-loop control system. An optical tracking system (Optotrak Certus, Northern Digital, Ontario, Canada) provided position feedback to determine the displacement required by each muscle to initiate and continue movement of the joint, while the muscle force was recorded [See Figure 11]. The optical tracking system also tracked the relative positions of the ulnar shaft, olecranon fragment and fracture plate. The test was repeated with different masses attached to the cadaver hand (a distal fixture) to examine how load in the hand affects motion at the fracture site. Based on the protocol and testing checklist developed during the end of this study, a biomechanical testing of modern olecranon plates can be planned appropriately.

Figure 11: An Optotrak Certus (Northern Digital Inc) Motion Capture System Installed in the Biomechanics Lab at The MORE Foundation

Triceps brachii and brachialis, two muscles which cross the elbow, were loaded. Triceps was programmed as the primary controller of extension as it must overcome the weight of the distal arm in order to move the elbow angle from 90 degrees to 170 degrees; gravity and brachialis move the arm back such that the elbow angle is 90 degrees.

The primary elbow flexor, brachialis was programmed to act as a stabilizer of the joint, particularly at high extension angles. When brachialis and biceps pulled across the elbow, a posterior sheer and rotation about the transverse axis were imparted to the olecranon that was resisted by the plate construct. Previous studies of olecranon fractures have not included any flexor tension across the joint, and rely solely on gravity to return the arm to flexion. However, even when the flexors are not firing to produce active contraction, they impart a passive tension across to the elbow joint which resists extension by the triceps and alters the joint reaction force.

This set-up and protocol validation study was important to standardize the following conditions for future biomechanical testing of olecranon fracture plating:

- the weight limits for testing and the number of cycles at each weights
- whether or not fatigue testing should be performed at physiologic loads or at the highest loading condition
- the rate of angular change to streamline the complete procedure with the same speed

These conditions were fixed with validation performed using four pilot specimens. The validation testing was also performed to verify the load capacity of elbow controller, function and use of the motors, kind of feedback control to be used for testing and creating the optimal coordinate system for elbow angle measurement and fracture fragment displacement. Figure 12 shows a process flow diagram of the procedure developed during this study.

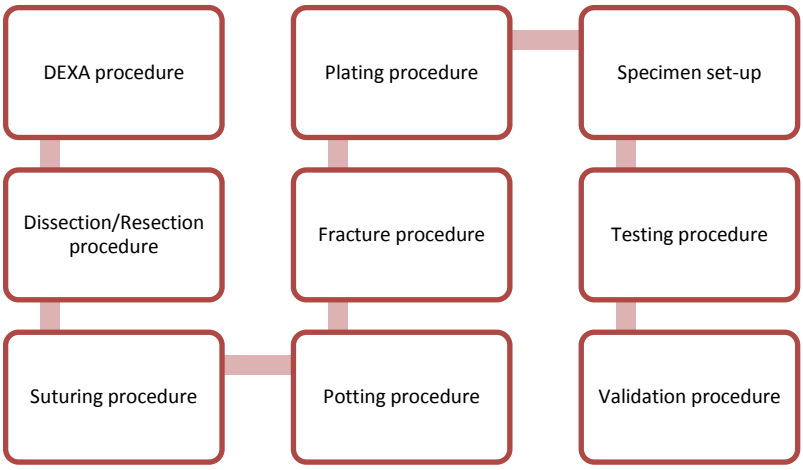

Figure 12:Process Flow Diagram of Olecranon Plating Study

CHAPTER 3

DEVELOPMENT OF METHOD AND PROCEDURES

After the feedback received from surgeon Dr. Paul Tornetta III, MD (Principal Investigator for this study) and brainstorming sessions with the team of MORE Foundation, design requirements were listed down to develop this novel procedure. [See Appendix A]

3.1 Design of Various Fixture

3.1.1 Design of The Main Frame

The main frame is a metallic fixture (aluminum), designed to support the forearm and its flexion-extension motion on the elbow controller. After several design revisions, feedback from the senior engineers and requirements of the study, a main frame was designed on SOLIDWORKS software [Figure 13] and 2D sketches are delivered to the professional workshop facility. [2D sketches in Appendix A]

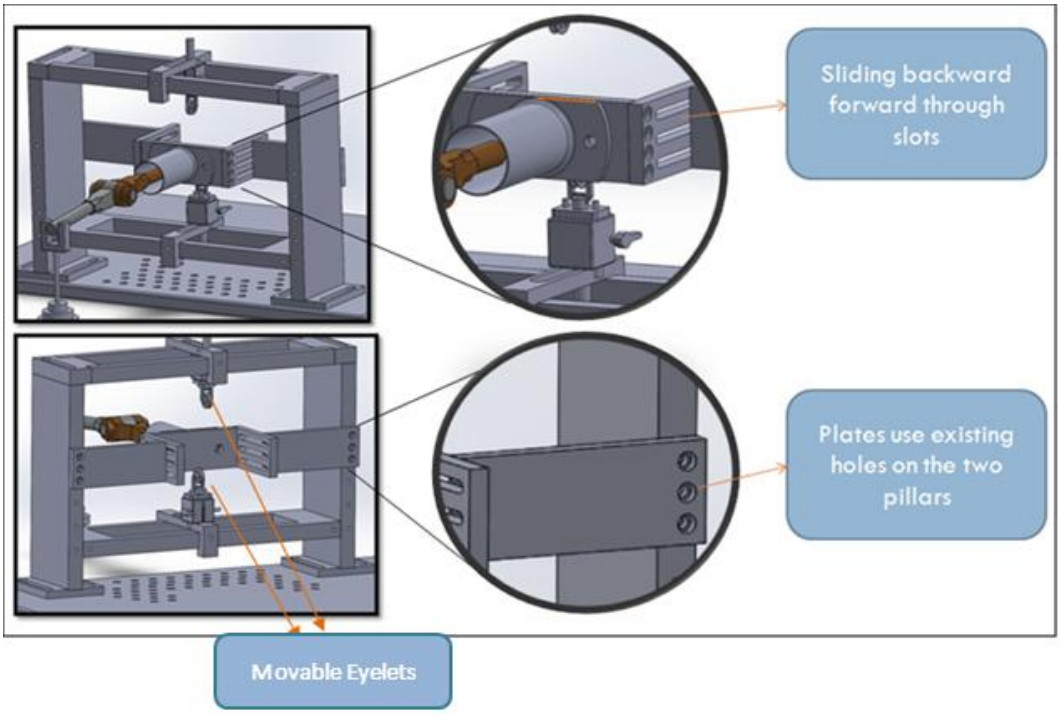

Figure 13: 3D Model Shows the Specialized Design to Make the Frame Flexible for Different Studies and Length of the Specimen

The pillar plate (Elb001A) was designed to use the existing holes in the pillar of the frame and can be moved up or down to maintain the height of the specimen and alignment of the cables with the actuators. The sliding mechanism in the slot-plates (Elb002A) provided flexibility to adjust the cable length. Once potted, the amount of cable needed to apply tension testing can be determined and, the plate could be locked in place. The main potting plate (Elb003A) held the humerus in the required position once the bone was potted in a humerus potting fixture. Figure 14 shows the machined main frame fixture with plates and eyelets.

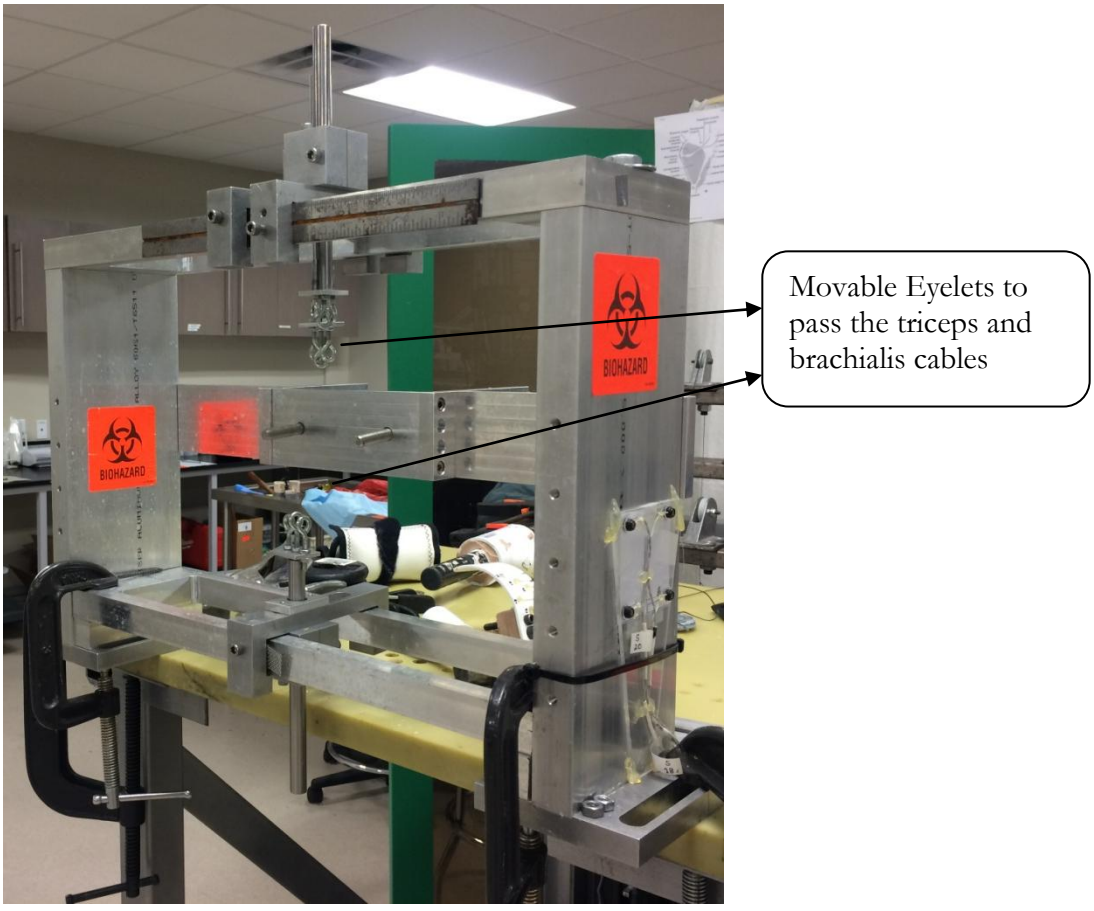

Figure 14: The Main Frame Set Up for Elbow Controller

3.1.2 Design of Radius-ulna Fixture

The distal fixture was created using PVC pipes and is of 17cm in size, though the size can be adjusted to make it longer [See Figure 15]. The proximal end is used to insert the radius-ulna of the specimen and the distal end is used to insert weights.

Figure 15: Distal Fixture to Accommodate the Length of Lost Forearm and Hand Formed Using Anthropometric Data

So, if the size of the forearm is 34 cm and the specimen is resected to 20 cm, 3 cm of the distal end of the specimen can be potted and insterted into the fixture. Therefore, it maintains the specimen length at 34 cm. This standard length has been calculated using antropometric data which needs height as an input value [see Table 3].

3.1.3 Design of Humerus Fixture

The humerus fixture is a 10 cm long fixture designed with PVC pipe and Bondo® mix to fix the humerus of the elbow specimen [See Figure 16]. It has two holes on the superior and inferior side, which will be used in digitization and defining the humeral shaft axis.

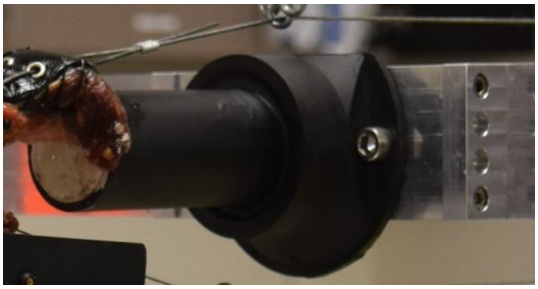

Figure 16: Humeral Fixture which Attaches on Main Frame and Keeps the Elbow in a Position where Triceps has to Maintain Maximum Load

3.2 DEXA Procedure

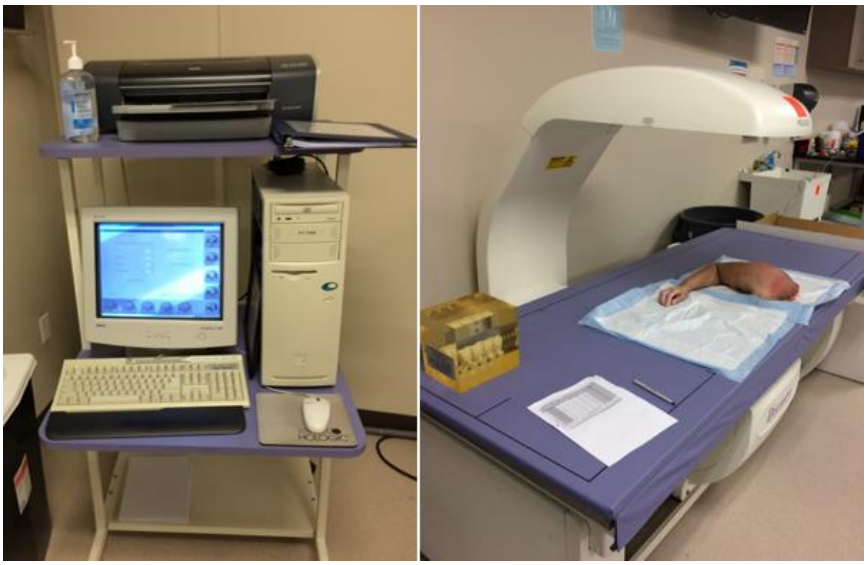

Figure 17: Hologic QDR DXA system setup in the Biomechanics lab of The MORE Foundation; A Cadaver Forearm is Lying with Right Orientation for Scanning Purposes A. Image of Computer that Runs the Procedure and B. Image of a Scanner that has the X-ray Source

Analysis of Bone mineral density (BMD) was performed on all specimens using Hologic QDR DXA system.

T- scores	Diagnosis
> -1.0	Normal density
-2.5 to -1.0	Osteopenia
< -2.5	Osteoporosis

Table 1: Diagnosis of Bone Density Based on T-Scores

All DXA results were determined to be appropriate based on age-, race-, and sex-matched controls. Figure 18 shows a typical scan of the section of the bone where the density measurement has been performed, values of bone mineral density (BMD) and t-scores [See Table 1]. The specimens were a mix of osteoporotic, osteopenic and normal BMD and post DEXA the reports are saved for reference.

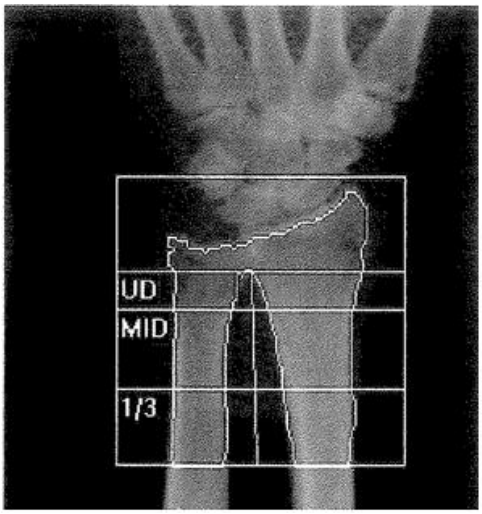

DXA Results Summary:

Radius + Ulna	Area (cm^2)	BMC (g)	BMD (g/cm^2)	T - Score	PR (%)	Z - Score	AM (%)
UD	4.01	1.08	0.268	-2.8	65	-1.9	74
MID	5.94	2.38	0.401	-3.5	68	-2.2	78
1/3	5.74	2.80	0.488	-3.4	71	-2.1	80
Total	**15.69**	**6.26**	**0.399**	**-3.2**	**71**	**-1.9**	**80**

Total BMD CV 1.0%
WHO Classification: Osteoporosis
Fracture Risk: High

Figure 18: A Typical Scan Shows all the Information From BMD and T Scores, also Shows the Diagnosis Automatically; In this Case T-Score is -3.2 hence a Case of Osteoporosis

3.3 Dissection and Resection of Specimen

Materials used were: Scalpel blade size 10 and 15, tweezers, and curette. Dissection of the arm included removal of all the soft tissues except triceps, brachialis, elbow capsule and radio-ulnar interosseous membrane [See Figure 18]. The specimens were free of evidence of previous surgery and preexisting pathologic conditions.

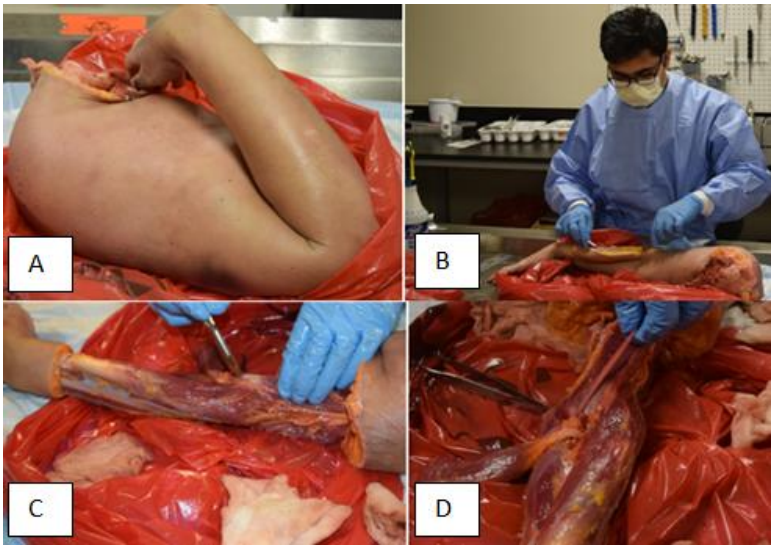

Figure 19: Dissection Day Included Thawing of the Arm for a Day and Dissection with Proper PPE A. A Thawed Arm Lying on the Dissection Table, B. Dissection Starts with Skin and Fat Removal, C. Identification of Brachialis and Triceps Insertion Points D. Separation of Brachialis and Triceps Muscle and Removal of all other Soft Tissues.

For resection, arms underwent transhumeral amputation 4.7 in (12 cm) proximal to the medial epicondyle point and trans-forearm amputation 7.8 in (20 cm) distal to the tip of the olecranon process keeping elbow at 90 degree flexion [Figure 20]. (See checklist in the Appendix B for details)

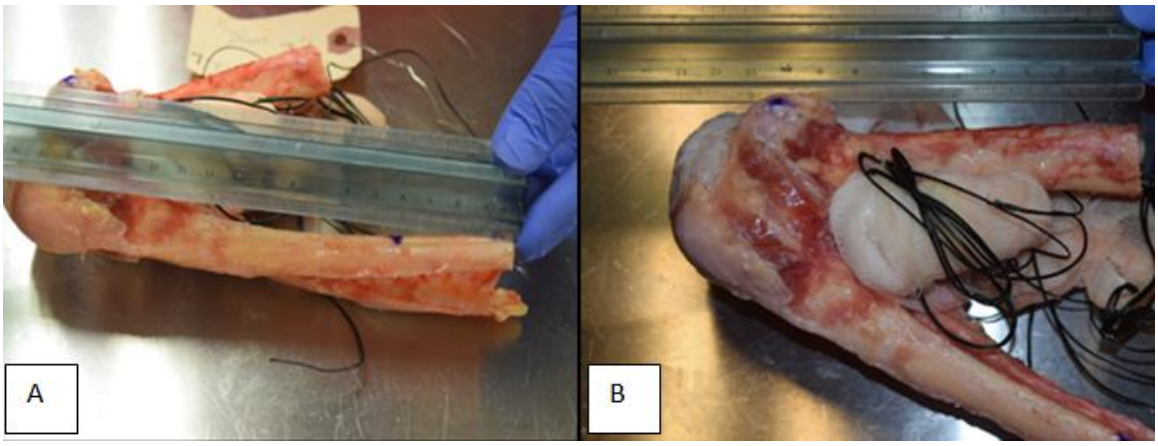

Figure 20: A. Resection of the Radius and Ulna (20 cm from Distal) B. Resection of Humerus 12 cm Proximal from Tip of Olecranon

3.4 Suturing Brachialis and Triceps Tendons

Brachialis tendon was sutured through the Krackow suturing technique [Figure 21] using fish cables (low stretch-high strength spectra cable). The technique grasps either a tendon or fascia sheet or other soft tissue by parallel running locked sutures. These loops tighten and lock to stabilize their grasp on the tissue as the strands of the suture are pulled to remove slack, and later as the repair or reconstruction is stressed [22].

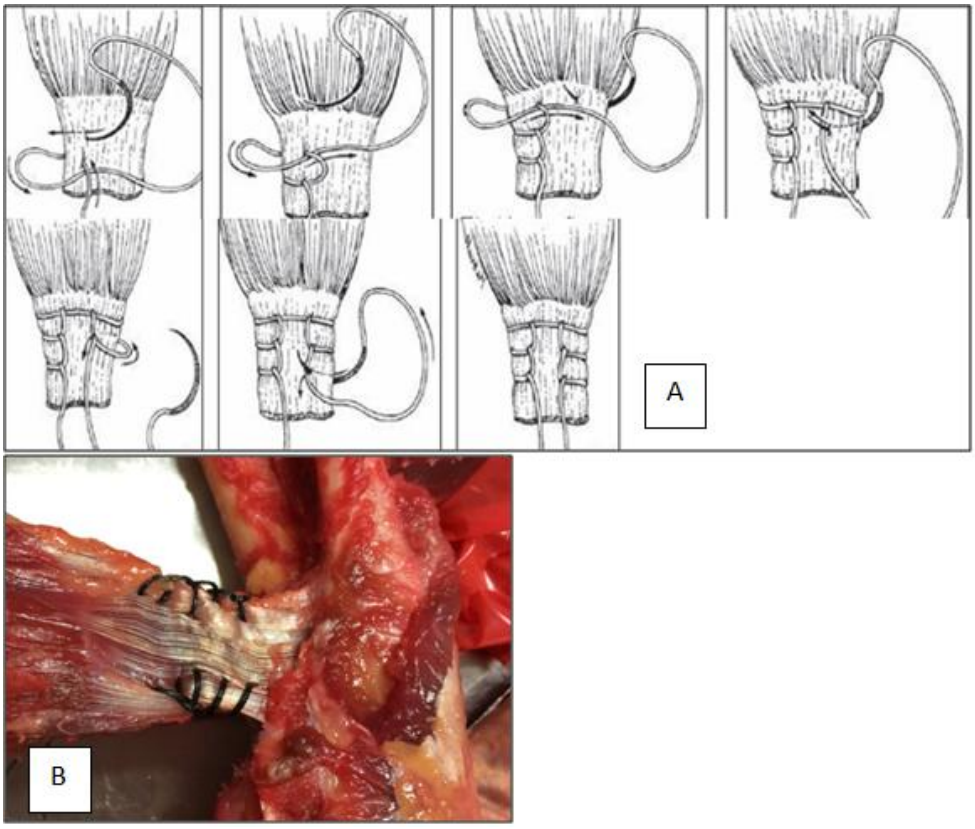

Figure 21: Krackow Suture Technique, A. Steps to Suture the Tendon [22] B. A Sutured Cadaveric Brachialis Tendon During the Experiment Following the Same Steps as in A

Suturing of triceps tendon was a challenging task from the very start of the study. Initially sutured with spectra cables, the knot failed several times as well as the tendon ruptured at several places during the first experimental set-up [see Chapter 4, Figure 34]. This was also a limitation of the set-up of King et al. as their suture attachment at triceps

failed between 300-500N [5]. This limitation was overcome by using leather belt strap with rivets sutured peripherally to the tendon and with steel cables passed though the eyelets [See Figure 22 and Figure 23].

Figure 22: Triceps Sutured with a Belt Strap and Krackow Suturing Technique, Steel Cable were Inserted Through these Holes

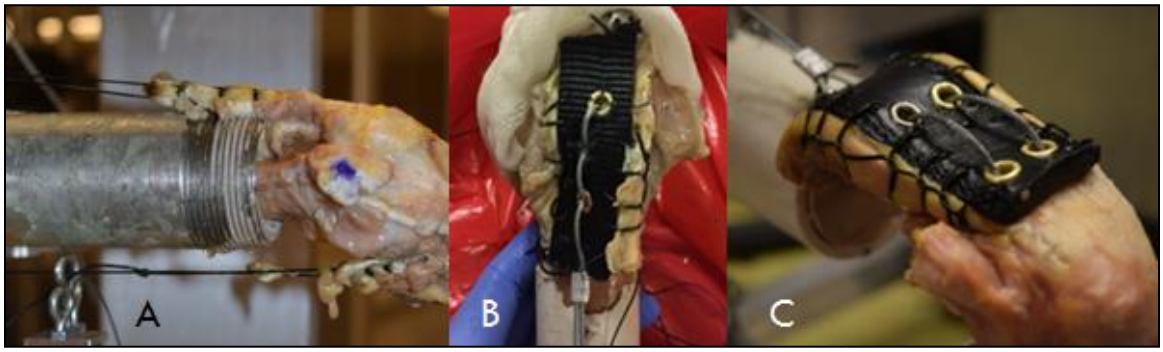

Figure 23: A. Sutured with only Spectra Cable in Pilot 1, B. Sutured Using Spectra Cable Nylon Strap, Rivets and Steel-wire (Single Row) in Pilot 2, C. Sutured using Spectra Cable Nylon Strap, Rivets and Steel-wire (Double row) in Pilot 3 & 4

3.5 Standardization of the Potting Procedure

A simple PVC pipe of 10 cm length was used to pot the humerus. The length of the humerus was standardized after several practice sessions with different pilot specimens as 2.36 in (6 cm) proximal to the medial epicondyle point. 6 Oz of Bondo® was used to pot the humerus and a wood screw was inserted into the humerus for better adhesion and rotational stability within the potting fixture [See Figure 24].

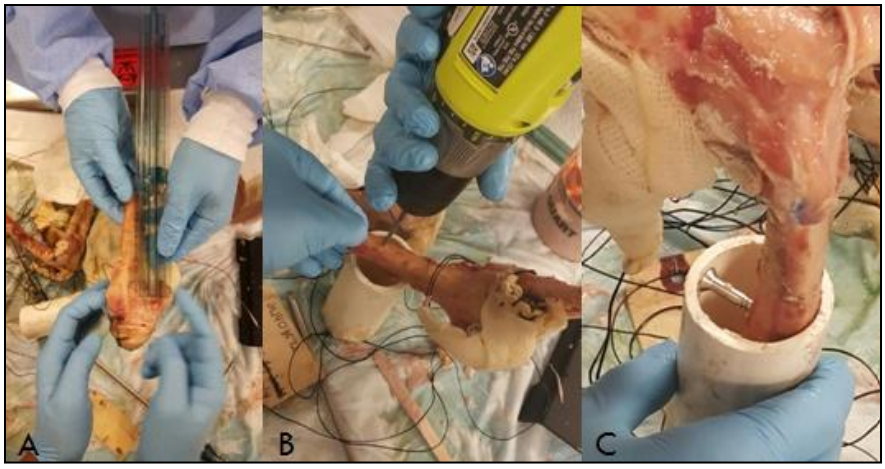

Figure 24: A. Measuring 6cm from the Epicondyles, Shaft Below that will be Inserted Inside the Pipe Fixture, B. A Wood Screw was Inserted for Better Adhesion and to Retain the Shaft at the Edge of the Pipe (C)

In a similar manner, radius-ulna were potted in a 6 cm long PVC cylinder with 4 Oz of Bondo® (See checklist in the Appendix B for details).

3.6 Defining the Coordinate System

The elbow joint is a hinge joint in which radius and ulna moves along the trochlea as a hinge and radius glides along the capitulum. The epicondyles of the humerus were used to define the center of rotation for the elbow.

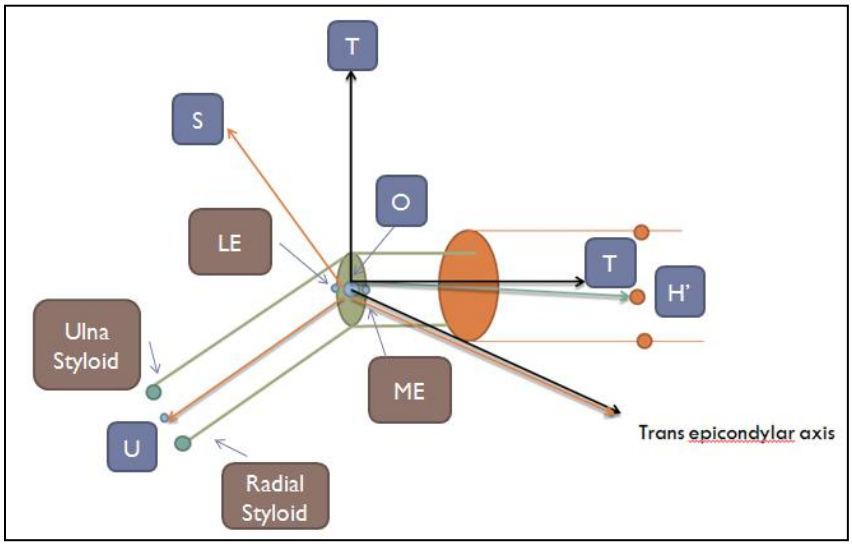

Figure 25: Defining the Coordinate System Using Landmark Points of Ulna, Radius and Humerus Bone

The trans-epicondylar axis was defined by connecting the digitized points (lateral and medical epicondyles) to form a common axis for both humerus and ulna-radius bone [See Figure 25]. The lateral and medial epicondylar (LE and ME) points were digitized to get the mid-point of the epicondylar axis which is also the center of rotation (O). These digitized points form the trans-epicondylar axis. The superior and inferior points at the humeral fixture were digitized to get the humeral fixture axis (OH'). The cross product of OH' and trans-epicodylar axis forms an axis OT which is perpendicular to the coronal plane of the humerus. Next, humeral shaft axis was obtained by the cross product of OT axis and trans-epicodylar axis. Similarly, two points were digitized on the ulna and radius called the styloid points. These points were digitized on the distal fixture (divoted clearly) which forms an axis OU', which is used to obtain an axis perpendicular to the coronal plane of the ulna called OS axis. The cross product of the OS and trans-epicondylar axis was used to obtain the ulna shaft axis OU. This approach makes a standardized method to set the coordinate system in all the specimens since it defines the axes through digitizing the common anatomical points. With the Euler sequence of rotations about anterior-posterior, medial-lateral and proximal-distal axes of elbow, the relative rotation of the reference frame ulna to the humerus was determined using rotation matrixes.

3.7 Standardization of the Length and Weight of the Specimen

3.7.1 Standardization of the Length

All the cadaveric arms were of different lengths for our study and that will be the case for the planned studies after this validation study. So one challenge was to make a fixture that can be adjusted according to the different length of the forearm. In our cadaver specimen database, the donors ranged from 59 to 73 inches in height (the information is provided by cadaver provider) therefore, the length of their arms differ. It is a challenging

task to make specific fixture for every specimen. Additionally, it is equally difficult to measure the length of their forearm accurately because of uneven soft tissue topography. Hence, an anthropometric calculation is performed to obtain the length of the different segment by using data [See Figure 26] from Physics of the Human Body, *I.P. Herman*, 2007.

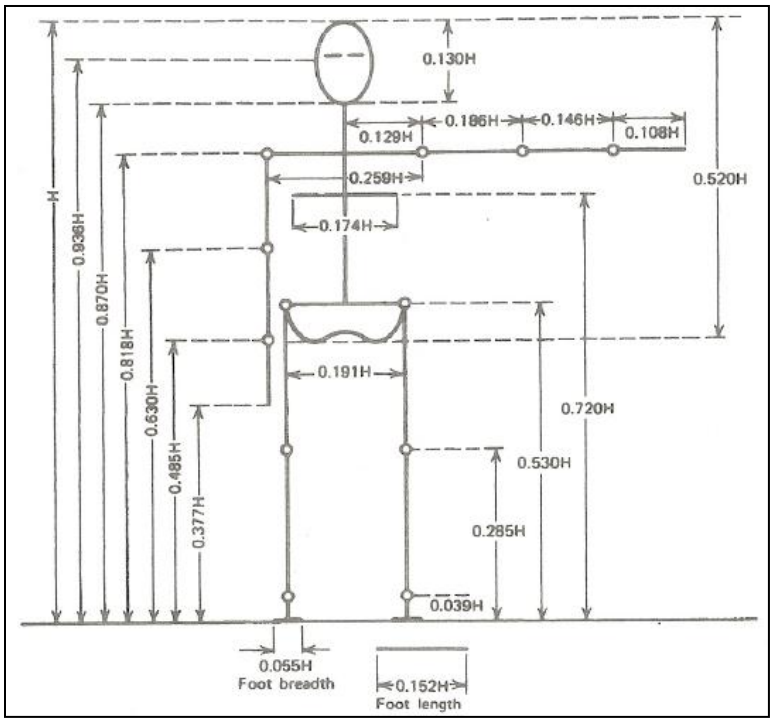

Figure 26: Body Segment Lengths Expressed as a Fraction of Body Height, H [Physics of the Human Body, I.P. Herman, 2007]

As the cadaver provider gives the donor summary including the length and weight of the donor, the segment length can be calculated through the above anthropometric data. For example, if a donor had a height of 69 inches (H), the length of its forearm (elbow to wrist) is 0.146 X H and hand (wrist to the tip of the longest finger) is 0.108 X H. Hence, the length of the forearm is 10 inches and hand is 7.5 inches. Since the experiment requires the specimen to hold weights in the hand, the weights should be held at the COM of the hand. Therefore, in the above example distance of the COM of the hand from the proximal joint is calculated using Table 2. As the length of the hand in the above example is 7.5 inches, the

COM of the hand is located 0.506 X 7.5 inches = 3.77 inches from the proximal joint. Similar calculations were performed on all the specimens in the database to get the average length [See Table 3]. The average length was then used in creation of a distal fixture (See Figure 27).

Segment	Definition	Segment Weight/ Total Body Weight	Center of Mass/ Segment Length		Radius of Gyration/ Segment Length			Density
			Proximal	Distal	C of G	Proximal	Distal	
Hand	Wrist axis/knuckle II middle finger	0.006 M	0.506	0.494 P	0.297	0.587	0.577 M	1.16
Forearm	Elbow axis/ulnar styloid	0.016 M	0.430	0.570 P	0.303	0.526	0.647 M	1.13
Upper arm	Glenohumeral axis/elbow axis	0.028 M	0.436	0.564 P	0.322	0.542	0.645 M	1.07
Forearm and hand	Elbow axis/ulnar styloid	0.022 M	0.682	0.318 P	0.468	0.827	0.565 P	1.14
Total arm	Glenohumeral joint/ulnar styloid	0.050 M	0.530	0.470 P	0.368	0.645	0.596 P	1.11
Foot	Lateral malleolus/head metatarsal II	0.0145 M	0.50	0.50 P	0.475	0.690	0.690 P	1.10
Leg	Femoral condyles/medial malleolus	0.0465 M	0.433	0.567 P	0.302	0.528	0.643 M	1.09
Thigh	Greater trochanter/femoral condyles	0.100 M	0.433	0.567 P	0.323	0.540	0.653 M	1.05
Foot and leg	Femoral condyles/medial malleolus	0.061 M	0.606	0.394 P	0.416	0.735	0.572 P	1.09
Total leg	Greater trochanter/medial malleolus	0.161 M	0.447	0.553 P	0.326	0.560	0.650 P	1.06
Head and neck	C7-T1 and 1st rib/ear canal	0.081 M	1.000	— PC	0.495	0.116	— PC	1.11
Shoulder mass	Sternoclavicular joint/ glenohumeral axis	—	0.712	0.288	—	—	—	1.04
Thorax	C7-T1/T12-L1 and diaphragm*	0.216 PC	0.82	0.18	—	—	—	0.92
Abdomen	T12-L1/L4-L5*	0.139 LC	0.44	0.56	—	—	—	—
Pelvis	L4-L5/greater trochanter*	0.142 LC	0.105	0.895	—	—	—	—
Thorax and abdomen	C7-T1/L4-L5*	0.355 LC	0.63	0.37	—	—	—	—
Abdomen and pelvis	T12-L1/greater trochanter*	0.281 PC	0.27	0.73	—	—	—	1.01
Trunk	Greater trochanter/ glenohumeral joint*	0.497 M	0.50	0.50	—	—	—	1.03
Trunk head neck	Greater trochanter/ glenohumeral joint*	0.578 MC	0.66	0.34 P	0.503	0.830	0.607 M	—
Head, arms, and trunk (HAT)	Greater trochanter/ glenohumeral joint*	0.678 MC	0.626	0.374 PC	0.496	0.798	0.621 PC	—
HAT	Greater trochanter/mid rib	0.678	1.142	—	0.903	1.456	—	—

Table 2: Distance of Center of Mass From Either Segment End, Normalized by the Segment Length [Physics of the Human Body, I.P. Herman, 2007]

	Specimen	Hgt (in)	Wgt (lbs)	Palm (from proximal) (in)	Total Length (Olecranon to Palm) (in)
1	GL1403572	65	180	3.55	13.04
2	GL1403558	63	110	3.44	12.64
3	GL1503589	66	123	3.61	13.24
4	GL1302560	73	340	3.99	14.65
5	GL1503600	68	155	3.72	13.64
6	GL1403480	64	140	3.50	12.84
7	GL1402802	70	450	3.83	14.05
8	GL1504067	71	170	3.88	14.25
9	GL1503621	59	70	3.22	11.84
10	GL1302745	65	245	3.55	13.04
11	GL1504053	68	80	3.72	13.64
12	GL1503987	68	175	3.72	13.64
13	GL1503981	72	240	3.93	14.45
14	GL1503836	65	258	3.55	13.04
15	GL1503982	70	200	3.83	14.05
16	GL1503974	69	112	3.77	13.84
	Average Length	**67.3**	**190.5**	**3.7**	**13.5**
	Size of the distal fixture should make the total length of the specimen= 13.5 inches (~34 cm)				

Table 3: Average Length of Forearm and Hand After the Calculations Performed Using Anthropometric Data

Figure 27: Designed Distal Fixture to Compensate the Dissected Ulna-Radius Bone and Hand

3.7.2 Supplemental Weight Calculations

Since all the soft tissues were removed from the cadaveric arm during the dissection, the muscle mass was estimated in order to provide a supplemental weight to simulate the weight of the intact forearm. The anthropometric data [See Table 2] from the Physics of the Human Body, *I.P. Herman*, 2007 was used to estimate the amount of the lost muscle mass and summarized in Table 4.

S.No	Specimen	Hgt (in)	Wgt(lbs)	Forearm Weight (lbs)	Hand Weight (lbs)	COM of Forearm (in)	COM of Hand (in)
1	GL1403572	65	180	2.9	1.1	4.1	3.6
2	GL1403558	63	110	1.8	0.7	4.0	3.4
3	GL1503589	66	123	2.0	0.7	4.1	3.6
4	GL1302560	73	340	5.4	2.0	4.6	4.0
5	GL1503600	68	155	2.5	0.9	4.3	3.7
6	GL1403480	64	140	2.2	0.8	4.0	3.5
7	GL1402802	70	450	7.2	2.7	4.4	3.8
8	GL1504067	71	170	2.7	1.0	4.5	3.9
9	GL1503621	59	70	1.1	0.4	3.7	3.2
10	GL1302745	65	245	3.9	1.5	4.1	3.6
11	GL1504053	68	80	1.3	0.5	4.3	3.7
12	GL1503987	68	175	2.8	1.1	4.3	3.7
13	GL1503981	72	240	3.8	1.4	4.5	3.9
14	GL1503836	65	258	4.1	1.5	4.1	3.6
15	GL1503982	70	200	3.2	1.2	4.4	3.8
16	GL1503974	69	112	1.8	0.7	4.3	3.8
Average		**67.25**	**190.5**	**3.0**	**1.1**	**4.2**	**3.7**
						From proximal	
The average weight of the lost musles and bones (Forearm)= 3 lbs and position= 4.2 inches from proximal							
The average weight of the lost musles and bones (Hand)= 1.1 lbs and position= 3.7 inches from proximal							

Table 4: Supplemental Weight Calculations Using Anthropometric Data Table for Masses and Mass Densities of Body Segments

CHAPTER 4

VALIDATION OF THE EXPERIMENTAL SETUP

Before starting the pilot tests, a layout of all the requirements [see appendix B] for the successful validation of the testing system, fixtures and procedure was created. Based on these requirements, design objectives were set so that all these requirements could be met in the pilots. Each experimental set-up was pilot tested and evaluated based on these design objectives. A checklist [see appendix B] was then created based to determine which set-up met all the design objectives.

4.1 Design Objectives

Design Objective 1. Reproducibility:

A. Effective method for digitization: Identify and fix the bony landmark on the bone for digitization so that it can be repeatable in all the specimens in further studies.

B. Reproduce muscle loads: The system should reproduce results from trial to trial for a specimen with respect to loads.

Design Objective 2. Standardization of the length of the forearm: The forearm length of different specimens may result in differences in the evaluation of displacement at the fracture site. Hence, the length of the forearm is required to be standardized.

Design Objective 3. Simulate supplemental weight of the forearm and hand: The forearms from different donors have different weights. In order to have the same effect at the fracture site, the supplemental weight is required to be standardized.

Design Objective 4. Set-up and techniques must be stable and run with low load fluctuations at higher loads: The experimental set-up must be designed in such a way that the weights of 3.75 -5 lbs at the hand can be tested successfully for multiple cycles. At higher loads, fixtures and suturing techniques must function uninterrupted and must not fail catastrophically.

Design Objective 5. Determine the maximum weight that load cell can sustain: Amount and increments of weight, number of cycles at each weight, and range of motion must be specified.

After setting the above objectives, four different cadaveric arms were tested on the feedback controller to validate and achieve our design objectives. An iterative process was followed where shortcomings and failures in each pilot testing were noted, new ideas and approaches were identified and implemented in the further pilots. Hence, the final pilot was run with all changes, best techniques and improved deigns in an attempt to meet the full set of design objectives. Figure 28 describes the flow diagram of the validation procedure.

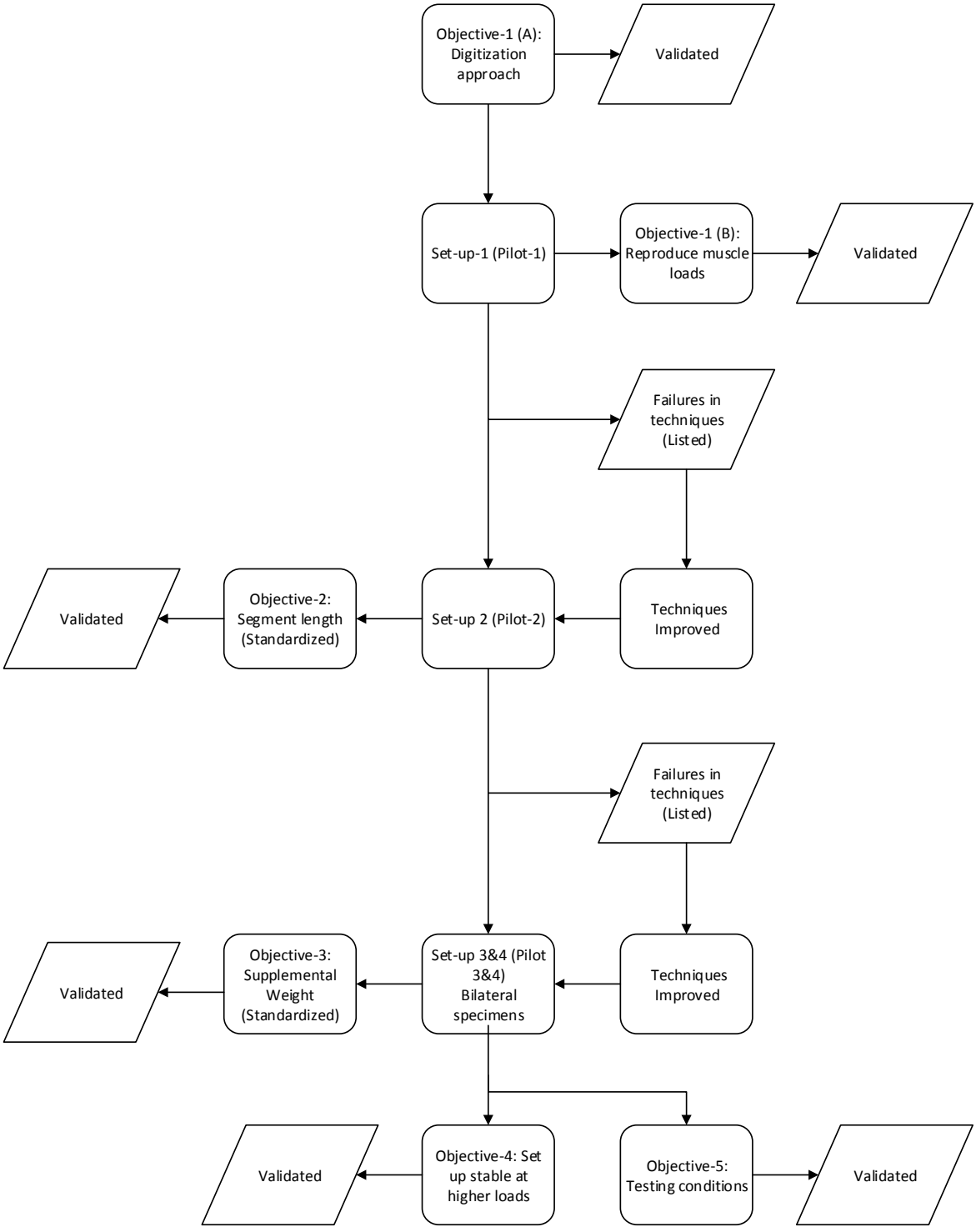

Figure 28: Flow Diagram Describing the Process of Validation the Experimental Set-Up Based on Design Objectives

4.2 Results

Design Objective 1. Reproducibility

1.A. Effective method for digitization: An approach must be identified to locate the same spot on the specimen for digitization as multiple trials are performed during an experiment and variations in the digitizing process would adversely affect the results. For instance, digitizing different points in the case of epicondyles may result in different set of angle calculations as epicondyles are responsible for defining the center of rotation (COR) of the elbow.

Digitization is a necessary step in defining the coordinate system and in the case of a cadaveric specimen, which is covered with soft tissue, an effective approach should be implemented in order to repeatedly identify the same bony landmark. Creating a divot or drilling holes in specimen can be an effective approach in digitization.

The digitization probe has a rounded end which must be held still while optical data is captured. Therefore, divots were created by drilling holes so that the rounded end of the digitization probe can remain still at one point (See Fig Figure 29).

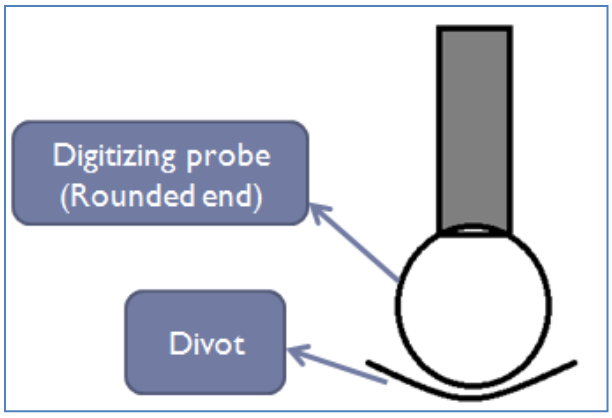

Figure 29: Spherical Geometry on the End of Digitization Probe Fits in Appropriately in Divot or a Hole

To evaluate this approach, data from 7 trials were collected in defining the global coordinate system (with three points in space) on the experimental set-up table (plastic material). As it is a solid platform, the points were well-defined and the probe could be placed in a highly repeatable manner and therefore the data that was captured became the best case scenario in comparing any other digitization points on the bone [See Table 5]. The average of the range values reported in Table 5 were 1.61mm, 0.44mm and 0.60mm for the X, Y, Z coordinates, respectively.

Global Landmark Points											
	Origin				**X+**				**XY+**		
	X	Y	Z		X	Y	Z		X	Y	Z
	320.40	-282.47	-1414.76		495.66	-279.31	-1473.05		437.26	-280.66	-1552.32
	320.48	-282.45	-1414.33		495.50	-279.65	-1472.38		437.37	-280.64	-1552.33
	320.46	-282.48	-1414.57		495.73	-279.45	-1472.76		437.31	-280.87	-1552.46
	321.79	-282.71	-1414.20		497.19	-279.79	-1472.17		438.77	-281.12	-1552.22
	321.78	-282.74	-1414.49		496.85	-279.85	-1472.54		438.62	-281.13	-1552.11
	321.97	-282.59	-1414.34		497.10	-279.70	-1472.21		438.83	-281.05	-1552.09
	321.86	-282.67	-1414.37		497.05	-279.80	-1472.27		438.63	-281.08	-1552.07
Avg	321.25	-282.59	-1414.44		496.44	-279.65	-1472.48		438.11	-280.93	-1552.23
SD	0.75	0.12	0.19		0.77	0.20	0.32		0.75	0.21	0.15
Range	1.57	0.29	0.56		1.69	0.54	0.88		1.57	0.49	0.38

Table 5: Divots were Created to Digitize the Global Landmark Points and Data was Collected in Seven Trials in Order to Validate the Effectiveness of Divot Approach

Medial and lateral epicondyle points were identified as the most prominent point on the bone, the points were drilled to create divots and marked with a surgical pen [See Figure 30]. The points were then digitized in three trials using digitization probe, data was captured and analyzed [See Table 6].

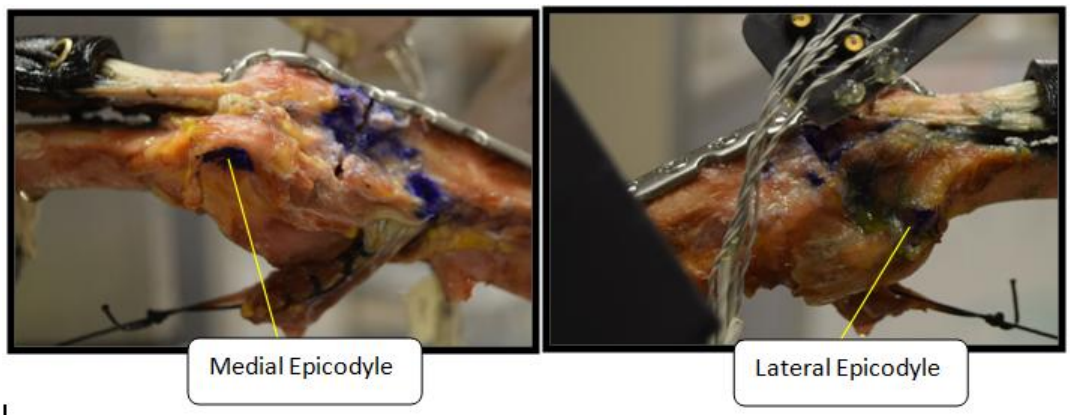

Figure 30: Divots were Made on the Landmark Points to Accurately Trace them for Digitization

Values in mm*							
EL co-ord. at Forearm frame				EM co-ord. at Forearm frame			
	EL_X	**EL_Y**	**EL_Z**		**EM_X**	**EM_Y**	**EM_Z**
Trial 1	19.72	92.97	-117.30	Trial 1	35.5	95.9	-58.5
Trial 2	20.98	93.73	-117.17	Trial 2	36.1	95.0	-57.5
Trial 3	19.25	93.62	-117.02	Trial 3	34.5	97.3	-57.3
Avg	19.98	93.44	-117.16	Avg	35.4	96.1	-57.8
SD	0.89	0.41	0.14	SD	0.8	1.2	0.6
Range	**1.73**	**0.77**	**0.28**		**1.56**	**2.28**	**1.12**

Table 6: Lateral (EL) and Medial (ML) Epicondyle Points were Digitized in Three Trials in Order to Validate the Effectiveness of Creating Divots

Range was calculated for both the cases and compared with the global landmark points data (best case scenario in optical tracking). While the y-coordinate range was greater than 2mm in the case of EM_Y, it is interesting to note that EM_X and EL_Z ranges were lower than all the x and z-coordinates of global landmark points; other range values were comparable to those from the global landmark points.

The approach was tested before beginning the experimental set-up (Pilot 1 to 4) and implemented further in all the pilots after successful validation.

4.3 Pilot-1 Experimental Set-up

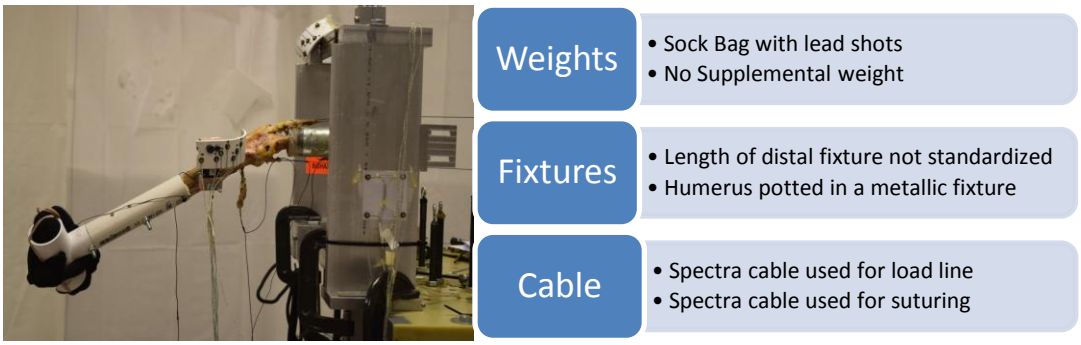

Figure 31: Pilot-1 Experimental Set-Up with Details about Fixtures

Design Objective 1.B. Reproduce muscle loads: The system should reproduce muscle load results for a specimen from trial to trial. Since the cadaveric specimen used in Pilot-1 was tested without creating fracture at the ulna, it is expected that there would be low trial-to-trial variability. The data was collected for 5 different trials for Pilot-1, Figure 32 shows graph between triceps load and angle from 5 to 75 degrees.

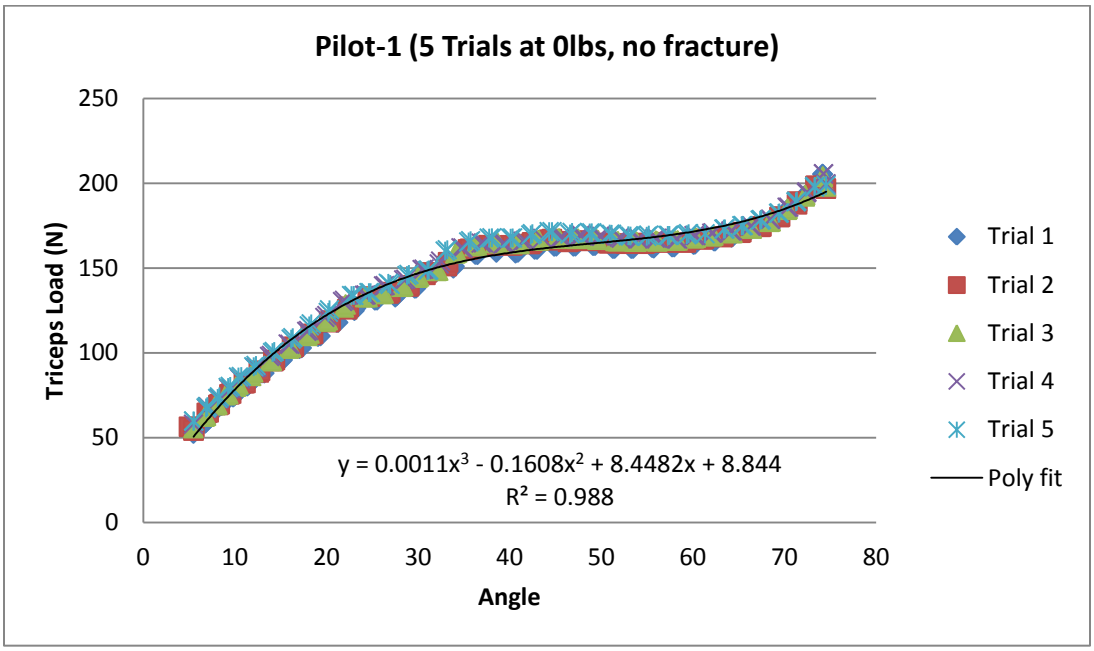

Figure 32: Results of Five Trials from 5 to 75 Degrees (Angle)

A third-order polynomial was used to fit the data and the result shows high R^2 value (0.988):

$y = 0.0011x^3 - 0.1608x^2 + 8.4482x + 8.844$

where y represents triceps load (N) and x represents angles (Degree)

To evaluate the variation in load data at different fixed angles, standard deviation and coefficient of variation was calculated from 5 to 75 degrees for 5 trials [See Table 7].

Coefficient of variation is less than or equal to 5% across the set of angles tested, which is a significantly lower value in load recording. It is interesting to note that at lower angle the variation is more, but at higher angle it consistently becomes better. The mean variability across the range of angles tested was calculated as:

$$\mathrm{Var}_{(\mathrm{mean})} = \sqrt{\frac{1}{N}\sum_{i=1}^{N}\sigma 2_i} \,/\, \frac{1}{N}\sum_{i=1}^{N}[X_i]$$

This value was determined to be 0.023, which indicates very low variability across the set of measurements.

	Load (N)							
Angle (deg)	**Trial 1**	**Trial 2**	**Trial 3**	**Trial 4**	**Trial 5**	**Mean**	**SD**	**CoefVar**
5º	52.3	56.3	55.6	57.9	59.7	56.4	2.75	**5%**
10º	73.8	75.9	80.0	79.0	80.2	77.8	2.82	**4%**
15º	95.8	95.7	102.4	105.2	100.8	100.0	4.16	**4%**
20º	109.9	118.0	119.2	121.9	123.8	118.6	5.37	**5%**
25º	130.9	133.0	132.8	134.1	135.4	133.2	1.68	**1%**
30º	138.1	139.7	145.0	149.1	146.2	143.6	4.57	**3%**
35º	150.9	160.9	159.1	161.8	165.3	159.6	5.36	**3%**
40º	158.7	163.4	164.1	164.5	167.5	163.6	3.19	**2%**
45º	162.8	167.0	167.2	168.1	171.4	167.3	3.09	**2%**
50º	163.1	164.7	166.6	168.7	170.0	166.6	2.79	**2%**
55º	162.0	164.7	166.1	167.6	168.7	165.8	2.61	**2%**
60º	163.8	165.1	167.4	169.1	170.2	167.1	2.68	**2%**
65º	168.6	170.8	170.6	171.9	174.9	171.4	2.31	**1%**
70º	184.0	180.3	184.3	185.8	182.5	183.4	2.07	**1%**
75º	199.8	196.8	198.0	199.5	198.7	198.6	1.21	**1%**

Table 7: Results of Coefficient of Variation for 5 Trials at Different Fix Angles and Data Recorded are Measurement of Load (N)

4.4 Discussion (Pilot-1)

Design objective-1 (B) was successfully validated through the Pilot-1 experimental set-up. This set-up failed to standardize the length of the forearm-hand and supplemental weight for different specimens. Additionally, several techniques failed during this experiment such as spectra cable as well as suturing technique. Therefore, this set-up failed to meet the other design objectives.

Problems encountered: At higher loads (>300N), fluctuation of 5N (error 2.8 %) was registered during capturing of load data (See Figure 43). The sock bag with lead shots was used to increase weights at the distal end of the specimen [See Figure 33]. This technique was inefficient as the sock bag was popping out of the T-shape fixture during flexion and extension motion of the arm. Also, the spectra cable failed in between 8th and 9th cycles when tested with 5 lbs of weight (400N) [See Figure 34]

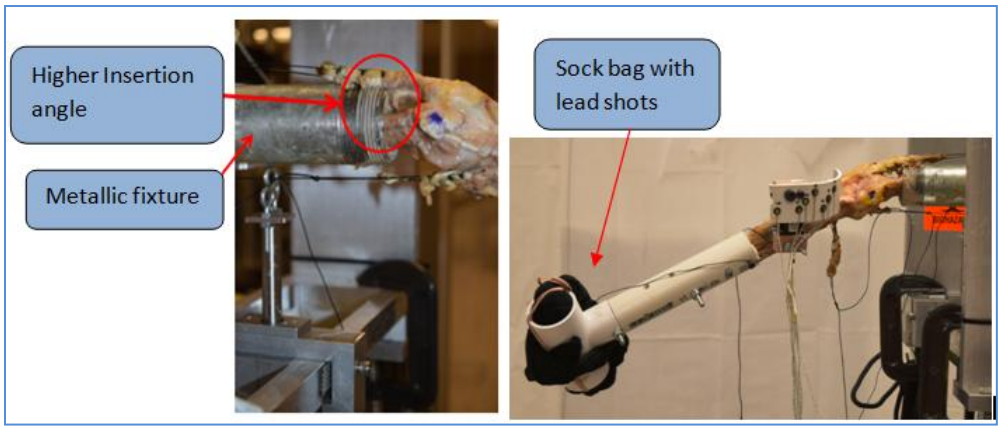

Figure 33: Humerus of Pilot-1 was Potted in the Center of a Cylindrical Metallic Fixture which Resulted in a Higher Insertion Angle

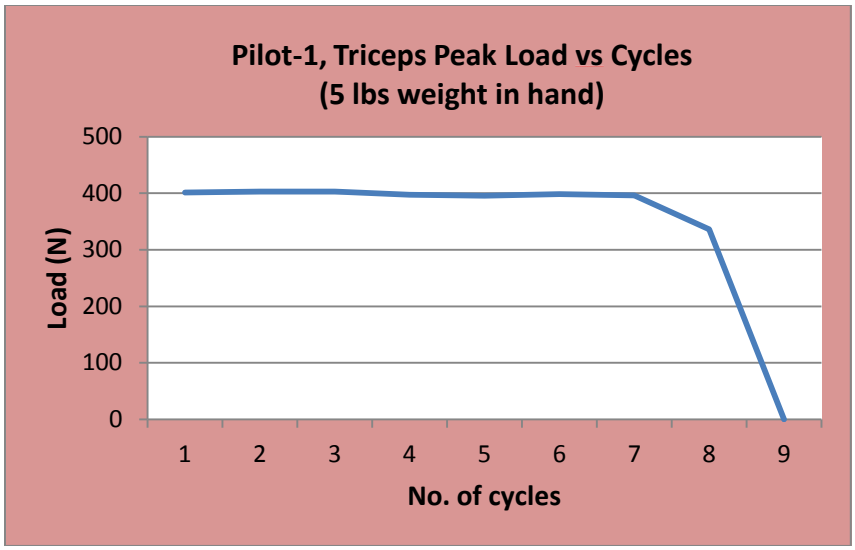

Figure 34: The Plot Shows Failure of the Spectra Cable to Maintain Load at 400N, Spectra Cable Snapped at 9th Cycle

After analyzing the failures in Pilot-1, Pilot-2 was tested with improved techniques as discussed in next page. Design objective 2 was validated using the anthropometric data table from Physics of the Human Body, *I.P. Herman*, 2007 by calculating the average length of forearm and hand of 16 specimens from the cadaveric database.

4.5 Pilot-2 Experimental Set-up

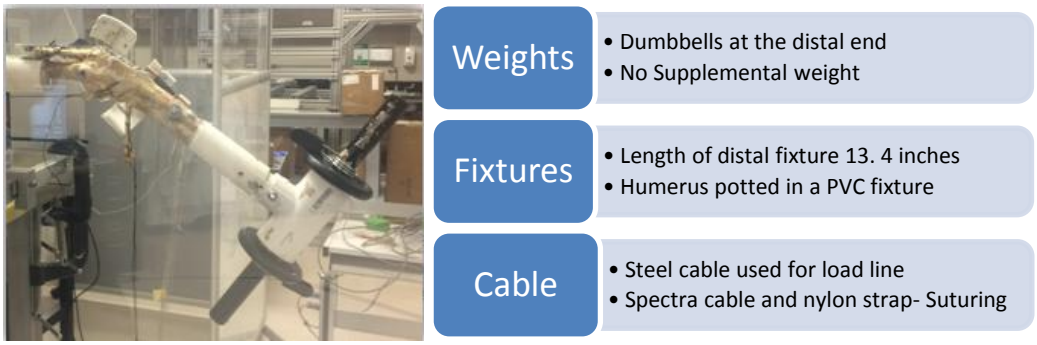

Figure 35: Pilot-2 Experimental Set-up with Details about Fixtures

Improved techniques:

a) Sock bag with lead shots was replaced with dumbbells

b) Length of the forearm was standardized based on the calculations performed through anthropometric data table

c) A PVC pipe fixture was created which replaced metal fixture for humerus potting

d) Potting method was improved by potting the humerus at edge of the cylindrical PVC fixture [See Figure 36]

e) Triceps tendon was sutured with nylon strap and steel cable.

Figure 36: Potting Technique of Humerus was Improved By Potting it at the Edge of The Fixture which in Turn Reduced the Insertion Angle

Design Objective 2. Standardization of the length of the forearm: The forearm length of different specimens may result in difference in the evaluation of displacement at the fracture site. Hence, the length of the forearm must be standardized.

Using the anthropometric data table from Physics of the Human Body, *I.P. Herman*, 2007, calculation was performed to find the forearm and hand length of all the specimens. Figure 37 describes the summary of the calculations.

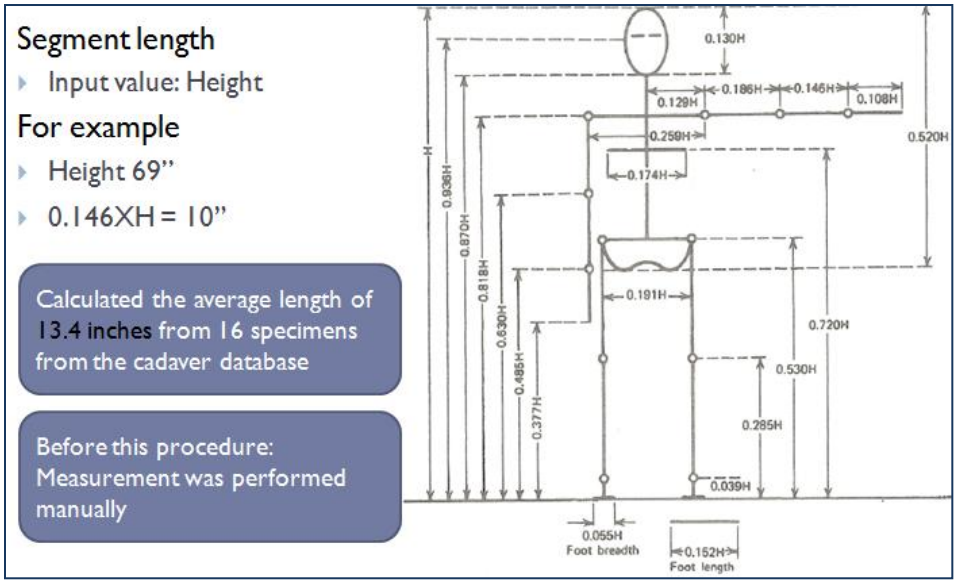

Figure 37: Average Length of the Forearm Calculated Using Anthropometric Data

After measuring the segment length of 16 specimens (cadaveric database), the average length of forearm and hand was calculated as 13.4 inches. Based on this length, the resection of the radius-ulna was fixed as 7.9 inches and 1.2 inches of distal bone was potted in a PVC fixture. Hence, a new distal fixture was created of size 6.7 inches [Figure 38]. This PVC fixture standardized the length of the complete forearm and hand for all the specimens.

Figure 38: Distal Fixture Created after Anthropometric Calculations of the Length of the Forearm and Hand of 16 Cadaveric Specimens from the Cadaveric Database

Standardization of length of the forearm and hand was a necessary step in order to have similar effect on the fracture site. A variable size distal fixture based on the different size of arms will have different moment arm. A higher moment arm may result in more forces at the fracture site and hence it will make the comparison between different specimens difficult.

4.6 Discussion (Pilot-2)

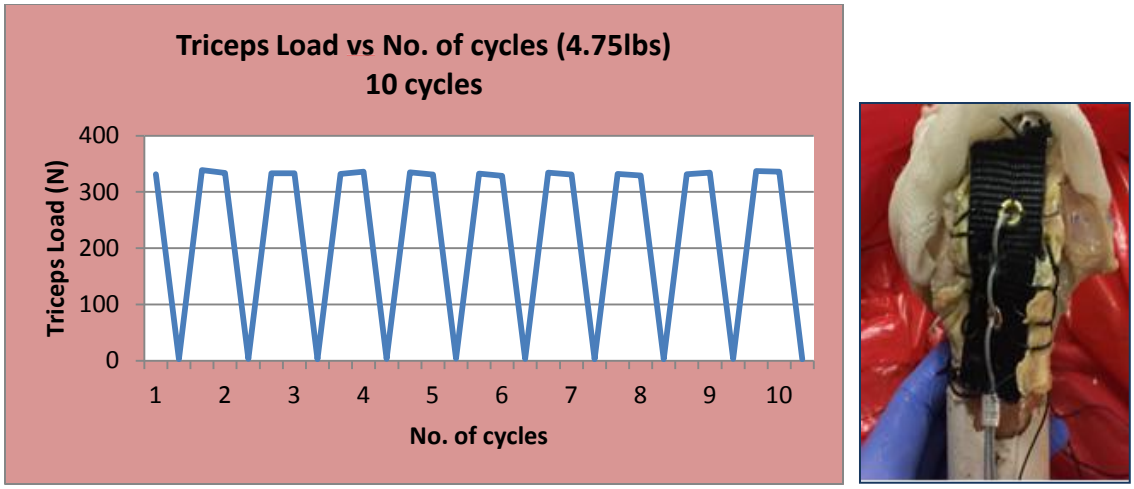

Figure 39: Pilot-2 was Tested with Different Weights at the Distal End; The Test was Stopped at 10 Cycles after Seeing Rupture at the Triceps Tendon

Pilot-2 was tested with different weights at the distal end for several trials. After tested with 4.75lbs at 10th cycle the test was terminated manually after seeing rupture at the triceps tendon (See Figure 39). Also, since the arm length, the supplemental weight should also be standardized. Although, the design **objective 2** was achieved in this pilot, several techniques needed improvement in order to achieve the rest of the design objectives.

Problems encountered: Rupture in triceps tendon was noticed after tested with 4.75 lbs. but during that time the specimen was run for several trials with weights in hand (1lb, 2.5 lbs). Also, the test was run without adding supplemental weight of lost muscle and soft tissue.

In order to meet the design objective 3, 4 and 5, Pilot 3&4 (bilateral arms) were run as explained in next section.

4.7 Pilot-3&4 Experimental Set-up

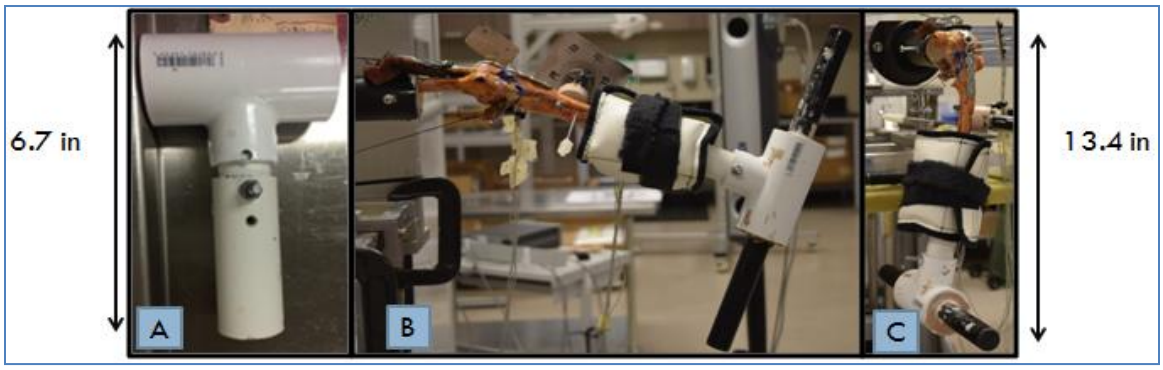

Figure 40: Pilot-4 Experimental Set-up with Details about Fixtures

Improved techniques [See Figure 41]:

a) T-shape fixture was potted with dumbbell rod

b) Belt straps with steel cables were used as a new suturing technique

c) Attached supplemental weight for lost muscle mass

Figure 41: Improved Suturing Technique at the Triceps Tendon, Leather Belt Strap was Used with Two Rows of Rivets to Attach with Steel Cable; T-Shape Potted with Dumbbell Rod

Design Objective 3. Simulate supplemental weight of the forearm and hand: The forearm from different donors has different weight. In order to have the consistent result at the fracture site, the forearm weight is required to be standardized.

As the first study to be performed after validation will test the effect of different plate constructs at fracture site as primary outcome, it is imperative that apart from surgical procedure and individual joint anatomy, all other factors that would result in fragment gapping or construct failure remain consistent.

The anthropometric data table was used to calculate the weight of the forearm and hand using 16 specimens from the donor database. The average weight of 4.2 lbs (including bone and muscle mass) was calculated using anthropometric data table from Physics of the Human Body, *I.P. Herman*, 2007 (See Table 4). The PVC fixture was potted with dumbbell bar which completed the lost weight of hand and 1.5 lbs of bag was wrapped at COM of forearm (calculated through anthropometric data, see Table 2).

Design Objective 4. Set-up and techniques must be stable and run with low load fluctuations at higher loads: The experimental set-up must be designed in such a way that the weights of 3.75 -5 lbs at the hand can be tested successfully for multiple cycles. At higher loads, fixtures and suturing techniques must function uninterrupted and must not fail catastrophically.

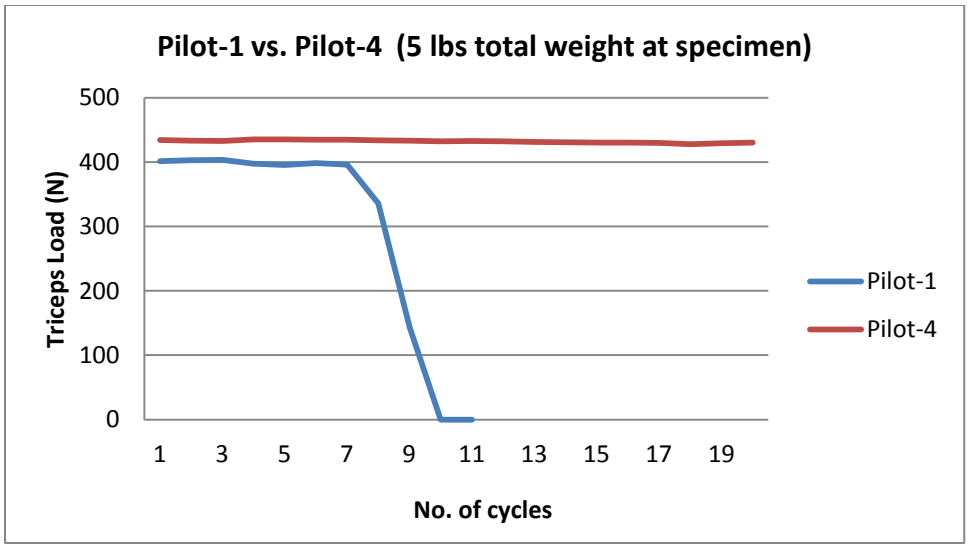

Figure 42: Difference in Survivability of Cable-Tendon Structure

During Pilot-1, the spectra cable snapped at various places and due to this reason testing at higher loads (~400N) failed. Figure 42 shows catastrophic failure of spectra cable to maintain load at 400N, yield point can be noticed between 7th and 9th cycle in the case of Pilot 1. However, the spectra cable was replaced with steel cable and belt strap suturing technique. The developed system and set-up (including fixtures, suturing etc) worked without any catastrophic failure throughout 240-300 cycles tested in the case of Pilot-3 and Pilot-4.

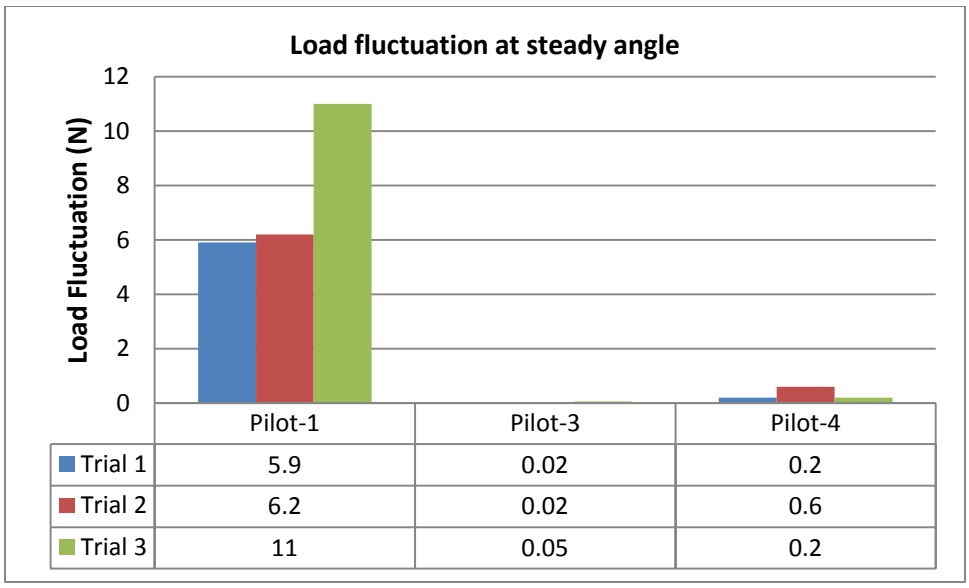

	Pilot-1	Pilot-3	Pilot-4
Trial 1	5.9	0.02	0.2
Trial 2	6.2	0.02	0.6
Trial 3	11	0.05	0.2

Figure 43: Load Fluctuation Recorded During a Steady Angle of 74 Degrees

Additionally, in Pilot-1 a load fluctuation of range of 5N (2.8% error) was observed during the data capturing at higher weight condition or higher load levels. This issue was resolved by tuning the angle control gain in the LABVIEW set-up and force fluctuation range was reduced to 1N (error 0.2%). Here, the load fluctuation is Max load - Min load recorded during a period of steady angle. Figure 43 shows the comparison of ranges of load fluctuation in three pilots at a steady angle of 74 degrees.

Design Objective 5. Determine the maximum weight that load cell can sustain: Amount and increments of weight, number of cycles at each weight, and range of motion must be determined.

The pilots were helpful in determining the maximum amount of weight that the load cell can handle. As the load bearing capacity of the load cell was 150lbf (close to 650N), the safer limit for testing was set at 500-550N.

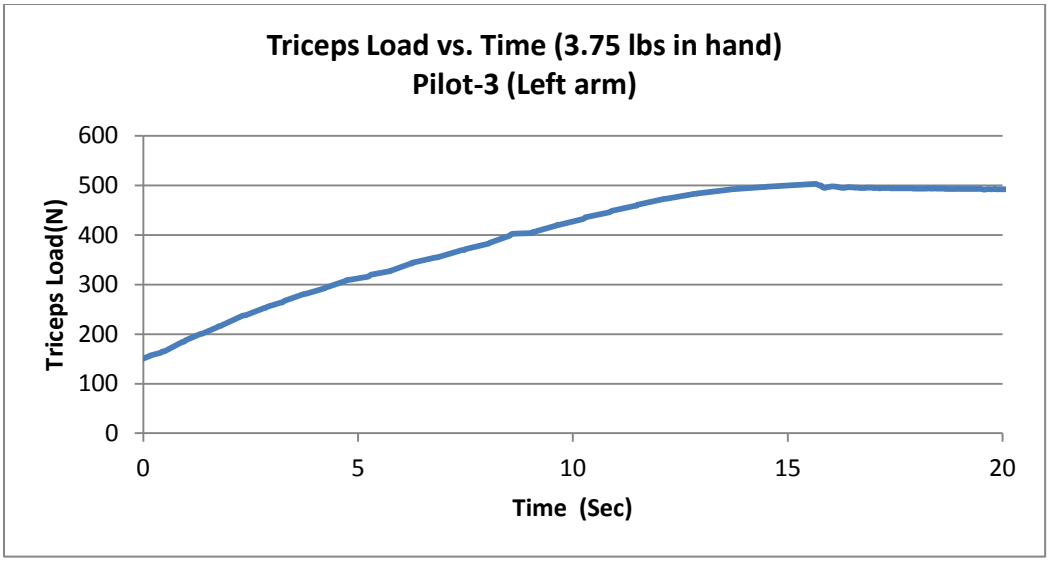

Figure 44: Shows the way the System Reacts after the Set Limit (500N Here); Table Shows that Loads Reaches Past 500N at 3.75lbs

In the LABVIEW set up, the load limit was fixed to 500N for Pilot 3&4. As the load reached 500N the system stops further testing and this way a safer set-up was developed [See Figure 44].

In order to confirm the range of motion (ROM) for testing, the Principal Investigator surgeon, Dr. Tornetta suggested to limit the extension to 75-80 degree from forearm at right angle to the potted humerus. Clinical failures usually occur due to repetitive loading across the fracture site [5] and not catastrophic failure. Additionally, during rehabilitation it is advised to do early range of motion and not to lift loads for a few months

post surgery. Therefore, the first round of testing consisted of 200 cycles at 0lb weight in hand (i.e. only weight of forearm and hand) condition. Hence, here a worst case testing was simulated with more cycles at ADL loads which shows realistic effects of construct fatigue in a clinical setting.

4.8 Discussion (Pilot-3 & Pilot-4)

Pilot 3 & 4 were bilateral specimens and were performed with only one difference in the set-ups and procedures. Both the arms were tested for 300 cycles, which was the maximum number of cycles tested. The COM of forearm was not at the calculated position in the case of Pilot-3, hence it did not met the **3rd objective**. But Pilot-4 was tested with supplemental weight at the right position [see Figure 40]. The complete set-up and techniques were stable, no catastrophic failure was observed throughout the cycle, which therefore achieved our **5th objective**. Pilot 4 met all the design objectives and as a result the testing conditions were fixed based on Pilot 4 for future studies.

Design Objectives	Pilot-1	Pilot-2	Pilot-3	Pilot-4
1. Reproducibility (A) Effective way of digitization	Pass	Pass	Pass	Pass
(B) Reproduce muscle loads	Pass	Pass	Pass	Pass
2. Standardizing the length of forearm and hand	Fail	Pass	Pass	Pass
3. Supplemental weight of forearm and hand	Fail	Fail	Fail	Pass
4. Set-up must be stable at higher loads	Fail	Fail	Pass	Pass
5. Max. weight at hand a load cell can sustain	Fail	Fail	Fail	Pass

Table 8: Summary of All Pilots and the Design Objectives they Met

The load cell limit in our current controller set-up is 150lbf (650 N) and pilot-4 validated that at 3.75 lbs weight the recorded maximum load is close to 550N. Hence, the experimental set-up (weights at distal end) must be tested with increment of weights till

3.75lbs. In order to test the fixation construct with higher loads either the load cells can be replaced with higher load cell limit or the load can be distributed in two actuator motors with the help of a pulley system. Table 8 shows summary of all the pilots from 1 to 4 with the design criteria they met. Initial pilots failed in most criteria but as the specimen progressed more of the criteria were passed each time, ending with validation that all criteria could be met. Therefore, this study developed a test platform to test olecranon fracture fixation and it was demonstrated to meet all of the specified design criteria.

CHAPTER 5

FUTURE WORK

The primary aim of the study was to develop and validate a novel protocol to test the olecranon fracture fixation using the modern olecranon plates in an upper extremity feedback controller. The current set-up is a worst case scenario in which the triceps is the primary loading muscle, through brachialis acts as stabilizer. This design set-up is a unique system that can replicate neuromuscular control of the joint using position feedback from the limb to drive tendon displacement. The validation of the complete set-up will eventually be used to evaluate the performance of olecranon plates with tines and without tines to fix a Mayo type IIA olecranon fractures. This study will use a combination of locked and non-locked screws on the proximal holes of the plate and hence four combinations will be tested on 16 paired cadaveric arms. This combination will evaluate the effectiveness of the tines with non-locked screws and whether expensive locked screws are necessary when tines provide the extra stability.

The other research question that could be answered with this type of set-up is to determine the amount of weight that can be safely lifted without causing significant fracture displacement. The information to be derived from this type of study can help surgeons to design a better rehabilitation plan for patients with fixation of MAYO Type IIA fractures. The use of functional muscle forces and dynamic range of motion in this set-up allows a more direct application of this biomechanical data to clinical decisions than is possible with load frame studies. The protocol can also be tuned to test the other ORIF technologies such as effectiveness of intramedullary nail as compared to locking plates. The current protocol was developed to test the MAYO type IIA fractures (Simple, stable) which is the most

common type is all olecranon fractures. A new fracture and fixation protocol is required to use it to compare the plate fixation for comminuted or unstable fractures.

In a similar manner, a study could be designed to analyze and compare the implants of lower extremity such as knee implants. The femur bone could be potted just like the humerus in this case and tibia-fibula can be moved in flexion-extension. The test set-up can be built to simulate the leg length and weight of the lost muscles in the similar manner (anthropometric data) it was calculated for elbow study.

REFERENCES

1. Rommens PM, Kuchle R, et al. Olecranon fractures in adults: factors influencing outcome. *Injury*. 2004;35:1149-1157

2. Nicolai Baecher, MD, Scott Edwards, MD. Olecranon fractures. J Hand Surg 2013;38A:593–604

3. Meredith L. Anderson, MD, A. Noelle Larson, MD, Sheri M. Merten, RN, and Scott P. Steinmann, MD; Congruent Elbow Plate Fixation of Olecranon Fractures; J Orthop Trauma; Volume 21, Number 6, July 2007

4. Byron E Chalidis, Nick C Sachinis, Efthimios P Samoladas, Christos G Dimitriou and John D Pournaras. Is tension band wiring technique the "gold standard" for the treatment of olecranon fractures? A long term functional outcome study. Journal of Orthopaedic Surgery and Research. 2008; 3:9

5. G. J. W. King, MD, P. N. Lammens, MD, A. D. Milne, BEng, J. H. Roth, MD, and J. A. Johnson, PhD. Plate fixation of comminuted olecranon fractures: An in vitro biomechanical study. J Shoulder Elbow Surg 1996;5:437-4 1

6. Prayson, Michael J.; Williams, John L.; Marshall, Michael P.; Scilaris, Thomas A.; Lingenfelter, Erich J. Biomechanical Comparison of Fixation Methods in Transverse Olecranon fractures: A Cadaver study. Journal of Orthopaedic Trauma; Vol. 11(8), November 1997, pp 565-572

7. Geert A. Buijze, Leendert Blankevoort, Gabrie¨lle J. M. Tuijthof, Inger N. Sierevelt, Peter Kloen. Biomechanical evaluation of fixation of comminuted olecranon fractures: one-third tubular versus locking compression plating. Arch Orthop Trauma Surg (2010) 130:459–464

8. Evan Argintar, MD, Benjamin D. Martin, MD, Andrea Singer, MD, Adam H. Hsieh, PhD, Scott Edwards, MD; A biomechanical comparison of multidirectional nail and locking plate fixation in unstable olecranon fractures; J Shoulder Elbow Surg (2012) 21, 1398-1405

9. Douglas T. Hutchinson, Md, Daniel S. Horwitz, Md, Gregory Ha, Md, Cameron W. Thomas, Bs, And Kent N. Bachus, Phd; Cyclic Loading of Olecranon Fracture Fixation Constructs; 2003 By The Journal Of Bone And Joint Surgery

10. Wilson J, Bajwa A, Kamath V, et al. Biomechanical comparison of interfragmentary compression in transverse fractures of the olecranon J Bone Joint Surg Br. 2011;93(2):245–250.

11. Matthew L. Hansen, MD, James C. Otis, PhD, Jared S. Johnson, MD, Frank A. Cordasco, MD, MS, Edward V. Craig, MD, and Russell F. Warren, MD; Biomechanics of Massive Rotator Cuff Tears: Implications for Treatment; J Bone Joint Surg Am. 2008;90:316-25

12. Christopher S. Bailey, Joy MacDermid, Stuart D. Patterson, and Graham J. W. King; Outcome of Plate Fixation of Olecranon Fractures; Journal of Orthopaedic Trauma Vol. 15, No. 8, pp. 542–548

13. David S. Wellman, MD, Lionel E. Lazaro, MD, et al; Treatment of Olecranon Fractures With 2.4- and 2.7-mm Plating Techniques; J Orthop Trauma; Volume 29, Number 1, January 2015

14. S.D.S. Newman, C. Mauffrey, S. Krikler; Olecranon fractures; Injury, Int. J. Care Injured 40 (2009) 575–581

15. Geert Buijze, MD, and Peter Kloen, MD, PhD; Clinical Evaluation of Locking Compression Plate Fixation for Comminuted Olecranon Fractures; J Bone Joint Surg Am. 2009;91:2416-20

16. Tobias E. Nowak & Klaus J. Burkhart et al. ; Locking-plate osteosynthesis versus intramedullary nailing for fixation of olecranon fractures: a biomechanical study; International Orthopaedics (SICOT) (2013) 37:899 – 903

17. Wei Chen, Qi Zhang, Zhiyong Hou and Yingze Zhang; The application of central tension plate with sharp hook in the treatment of intra-articular olecranon fracture; BMC Musculoskeletal Disorders 2013, 14:308

18. Sardelli M, Tashjian RZ, MacWilliams BA; Functional elbow range of motion for contemporary tasks 2011 Mar 2;93(5):471-7. doi: 10.2106/JBJS.I.01633

19. Hume MC, Wiss DA; Olecranon fractures: A clinical and radiographic comparison of Tension Band Wiring and Plate Fixation; Clinical Orthopaedics and Related Research, Feb 12 1991

20. Onstot Brian R., Jacofsky Marc C., Hansen Matthew L.; Muscle Force and Excursion Requirements and Moment Arm Analysis of a Posterior-Superior Offset Reverse Total Shoulder Prosthesis; Bulletin of the Hospital for Joint Diseases 2013;71(Suppl 2):S25-30

21. Onstot BR, Richardson N, Neelay RA, Jacofsky MC, Otis JC, Hansen ML; Deltoid Force and Excursion Demands of the Reverse Total Shoulder Prosthesis Compared to Massive Rotator Cuff Tear; Poster No. 1218; ORS 2012 Annual meeting

22. K.A Krackow, MD; The Krackow Suture: How, When, and Why; Management factorials in primary TKA; Sep 2008. Vol 31 Number 9

Other References:

23. http://www.ortovit.eu/ortopedie/trauma/tehnici/S&N/Tehnica%20operatorie%20PERILOC/OLECRANON%20SURGICAL%20TECHNIQUE.pdf

24. Andrew Jaczynski. M.S.E. Bioengineering, Arizona State University. Biomechanical analysis of reverse total shoulder arthroplasty.

25. Thompson, Jon. (2010). Netter's Concise Orthopaedic Anatomy (2nd Edition), Philadelphia: Saunders Elsevier

26. Neumann, Donald. (2010). Kinesiology of the Musculoskeletal System: Foundations for Rehabilitation (2nd Edition), Mosby/Elsevier

APPENDIX A

2D DRAWINGS AND PLATING PROTOCOL

1. 2D Drawing of Main Plate where Humerus Fixture Fits

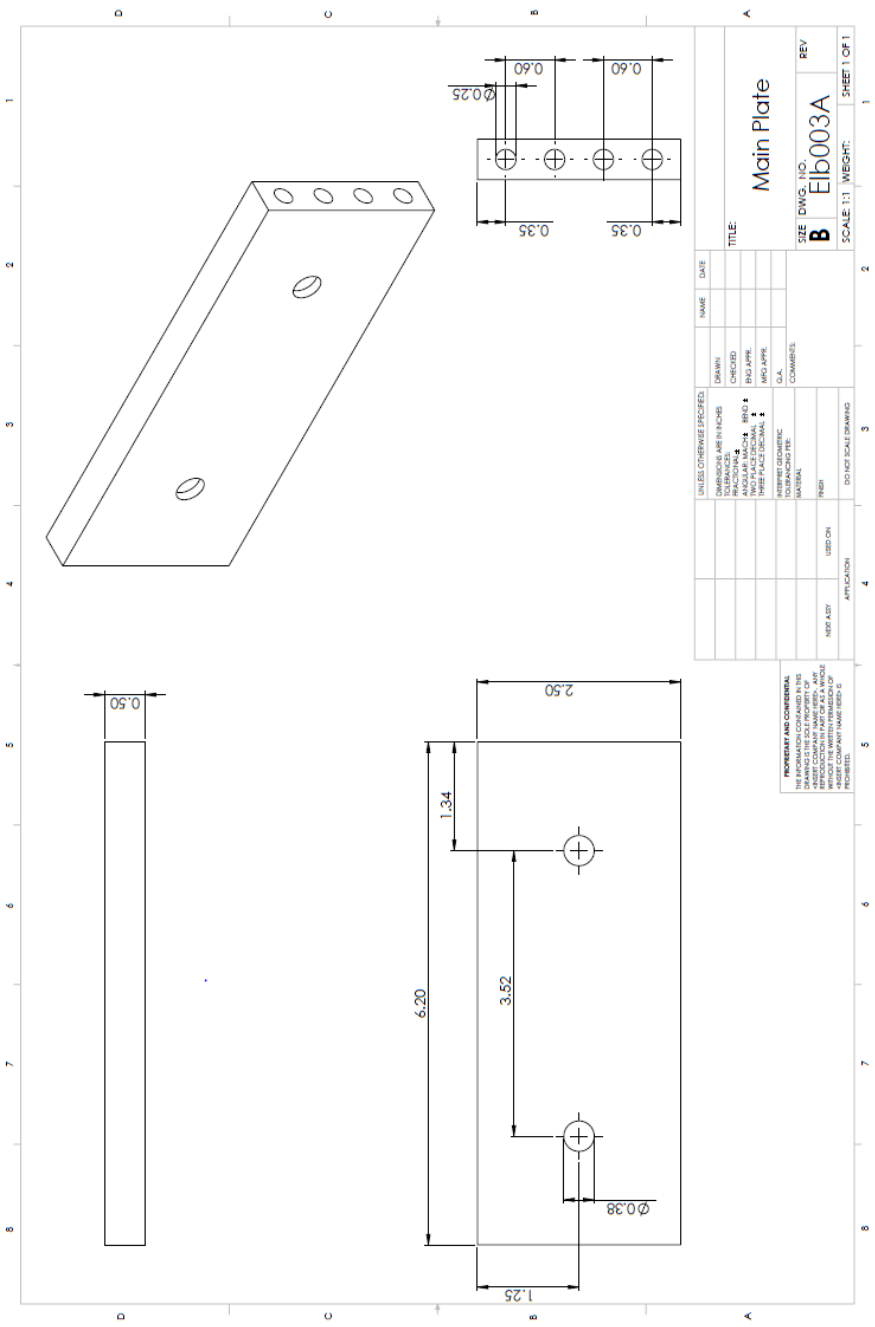

2. 2D drawing of Pillar plate which fits to the standing pillars of upper extremity controller

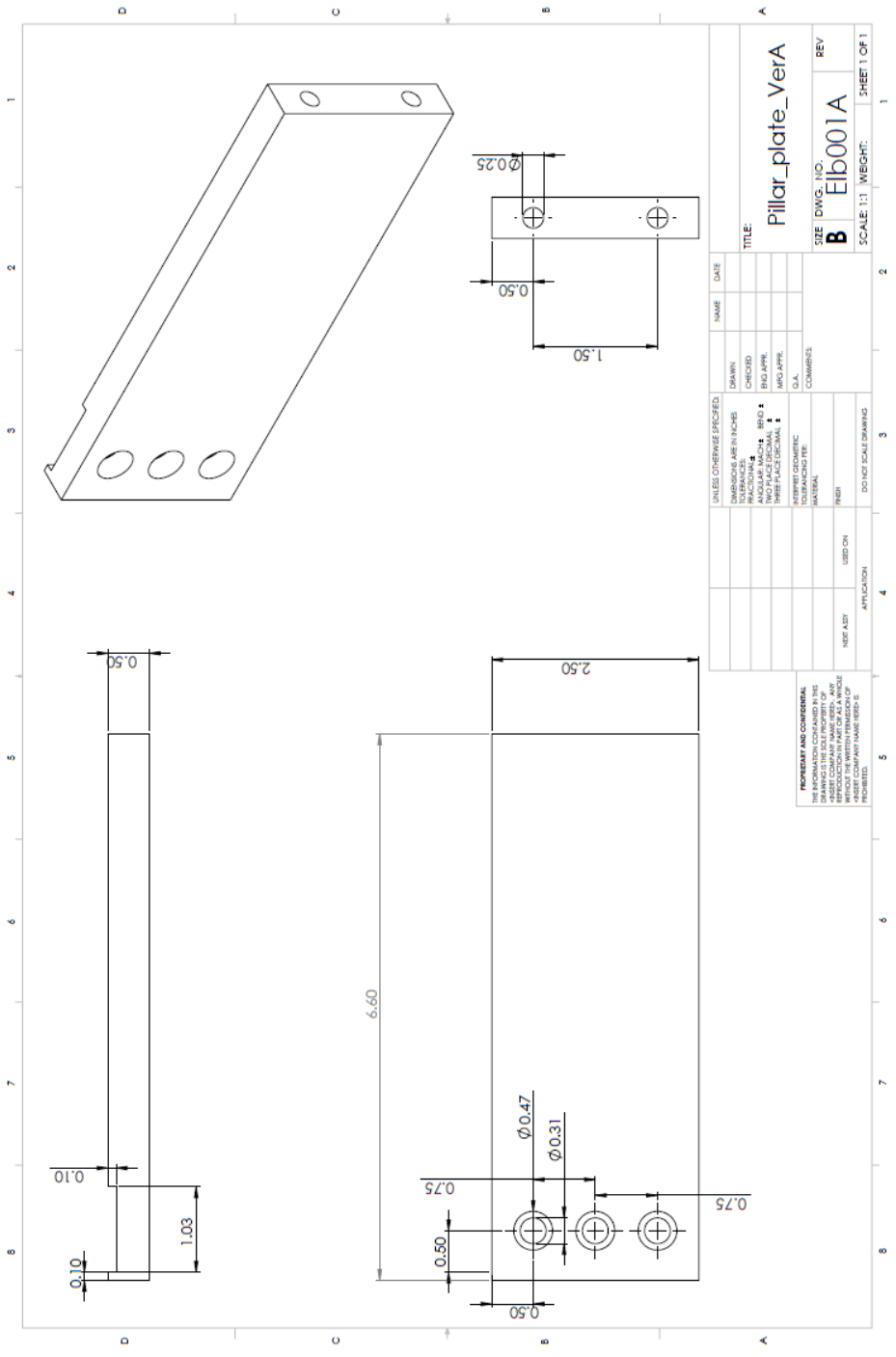

3. Fracture and plating procedure through saw bone

This procedure has been prepared with the help of Dr. Tornetta, who is the consulting surgeon for this study and Dr. Lee, a fellow from The CORE Institute. The procedure has been validated on a saw bone by following a series of steps to create fracture and fix the fracture through Smith and nephew instrumentation.

1. Materials required for plating

Required Instruments	**Size**	**Quantity**
Smith & Nephew olecranon plate	81 mm length	16
Surgical drill bit	2.7 mm diameter(Orange)	1
	2.0 mm diameter	1
K-wires	1.6 mm diameter	2
Non locking drill guide	2 mm X 2.7 mm	1
Reduction forceps (Tenaculum)		2
Depth gauge		1
Hex driver	3.5 mm	1
	2.0 mm	1
Locking drill guide	2.7 mm	1
	2 mm	1
Saw blade	0.8 mm thickness	1
Mallet		1

Bone tamp		1

2. Fracture creation

2.1 Landmark identification to perform osteotomy

2.1.1. From the deepest point of the semilunar notch of ulna, start osteotomy using a 0.8mm or less thick saw blade perpendicular to the long axis of the bone.

2.1.2. A radiograph of cadaver specimen should be used to identify the deepest point of semilunar notch or greater sigmoid cavity of ulna. Place the plate over the specimen and mark a line 2mm proximal from the 5th hole of the plate. Refer figure 1 and 4.

Note: The fracture line should be around 30 mm from the back of the plate and away from the tip of proximal articular screw.

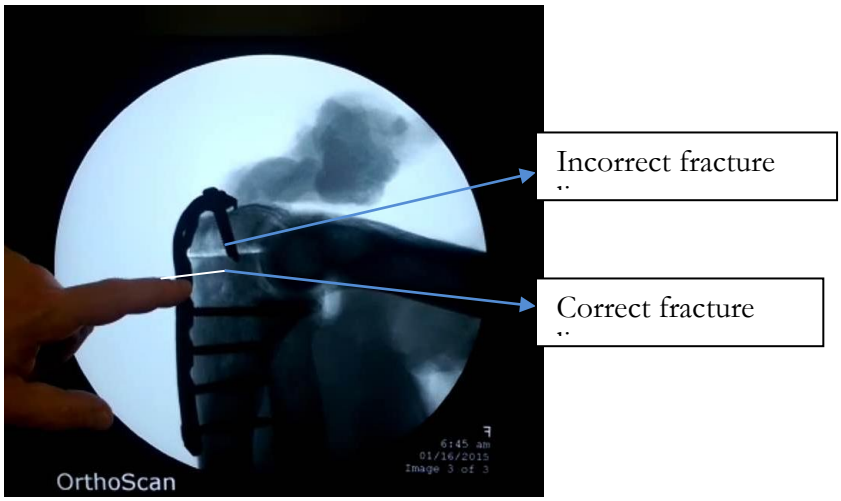

Figure 1: Hand in the Radiograph Indicates the Correct Site for the Fracture; Image Shows Incorrect Fracture Line which is Engaging with the Proximal Articular Screws

2.2. Reduction procedure for fracture fragment:

2.2.1 Make two cortical holes on the lateral and the medial aspect of the bone to reduce the fracture using 2 reduction forceps (tenaculum).

Note 1: The cortical holes should be made preferably before the osteotomy.

Note 2: Reduction aids should be placed so as not to interfere with final plate placement.

2.3. Placement of plate positioning K-wires

2.2.2 Insert two 1.6 mm diameter K-wires through the small holes on the proximal side of the plate inside the bone in the direction of impact and a little down. A pin collet can be a helpful tool during insertion of k-wire. Note: If possible see the progression of the K-wires under fluoroscopy.

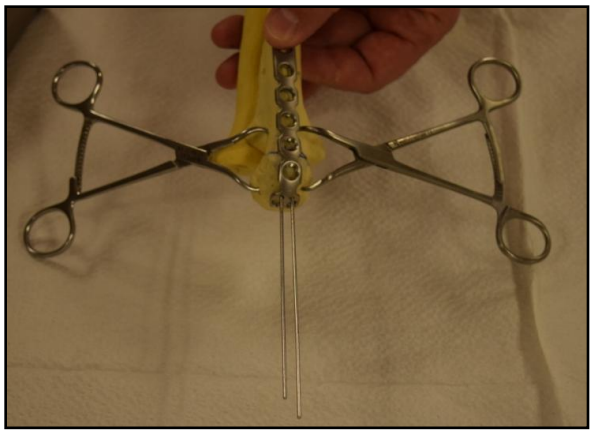

Figure 2: Bone after the Insertion of K-wires

2.4. Using mallet and bone tamp, tamp the plate down to the bone and across until tines engage into the triceps tendon.

Note 1: Be careful while tamping the plate as it could tilt if tamped on the region below the K-wires.

Note 2: Tamp every specimen with or without tines.

Figure 3: Tamping of the Plate Using Bone Tamp to Engage Tines

3. Plating technique

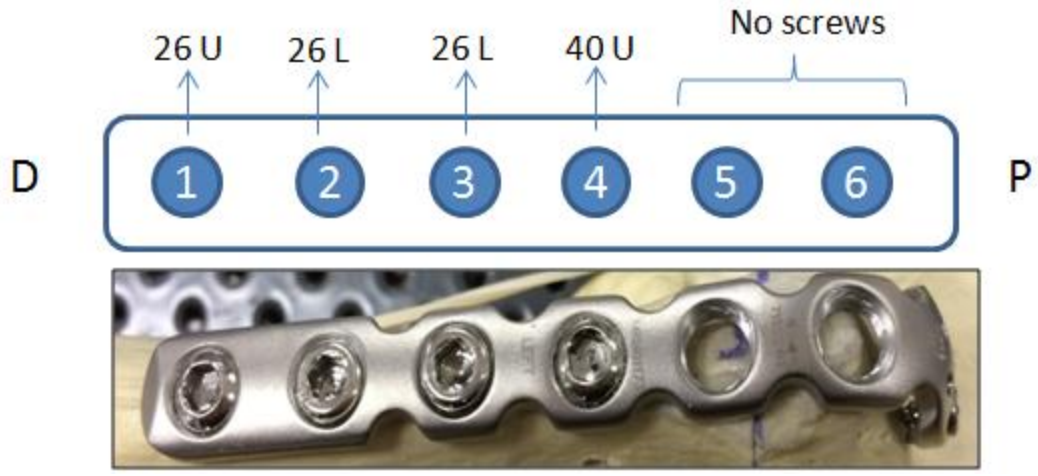

Figure 4: The Image Shows Sketch of Shaft Screw Holes of Plate where P Denotes Proximal, D Denotes Distal**,** L Denotes Locked And U Denotes Unlocked

3.1 Start with the distal most hole (Hole no. 1) for inserting a 26 mm self-tapping cortex screw.

Note: All screws (locked or unlocked) along the length of the plate will have 3.5 mm diameter

Figure 5: Circled screw is a 26 mm cortex screw inserted on the distal-most end of the plate

3.2 Take a 2.7mm diameter drill bit (identfiable by an orange ring) and drill into the bone with the help of 2.0mmX2.7mm **nonlocking drill guide**.

Figure 6: 2.0mmX2.7mm Unlocking Drill Guide**.**

Note: In our study, we have been taking a standardized screw length for all the specimen. Otherwise, the procedure requires the use of **depth gauge** to confirm the size of screw.

3.3 A 3.5 mm **hex driver** is used to advance the screw inside the bone using power drill and could be further advanced into the bone using the hand.

3.4 Previously placed K-wires in the posterior part of the olecranon need to be removed prior to insertion of the 40mm cortex screw (Hole no. 4). Refer Figure 4 to see the hole location.

3.5 Insert the next shaft screw in the hole no. 4 of the plate. The screw type is 40mm cortex screw, inserted in the same way as the first one.

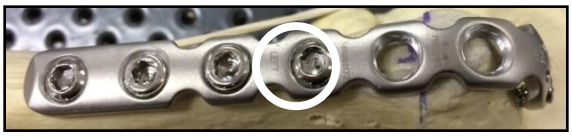

Figure 7: Circled Screw is a 40 mm Length Cortex Screw Inserted on the Distal-most End of the Plate

3.6 Two 26mm cortex locking screws are inserted in the hole no. 2 and 3 of the plate. Refer Figure 4 and 7 for screw location.

Note: These screws are always inserted perpendicular to the plate.

Figure 8: Shows the Olecranon Plate Inserted with Two Cortex Screws. Two Holes for Locking Screws are Indicated with a White Circle.

3.7 With 2.7mm diameter drill bit (with orange ring) and a **2.7mm locking drill guide**, holes are drilled perpendicular to the bone. This guide is necessary to insert the screws (with threaded head) in the accurate orientation.

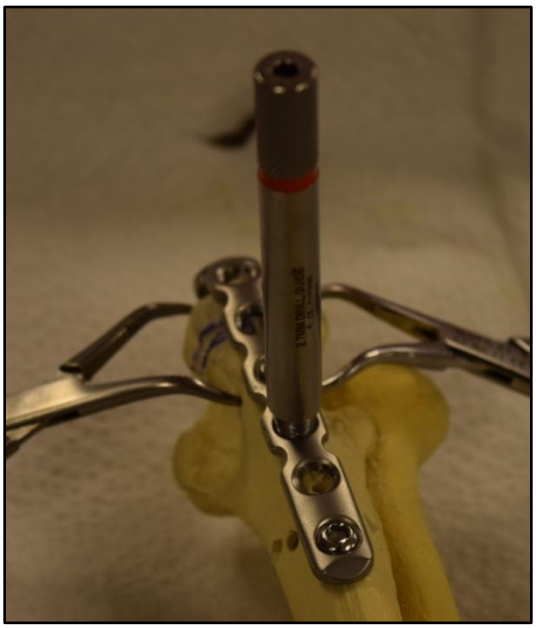

Figure 9: A 2.7 mm Locking Drill Guide is Used for the 26mm Cortex Locking Screws

3.8 A 3.5 mm **hex driver** is used to advance the screw inside the bone using power drill and could be further advanced into the bone using the hand.

3.9 The same steps are followed to insert the second 26mm cortex locking screw in hole no. 2 or 3. Refer Figure 4 for screw location.

3.10 After the insertion of the shaft screws, the 2.7mm(D)X20mm(L) screws are inserted in the olecranon fragment.

Figure 10: A Locking Drill Guide is Used to Drill Hole in the Olecranon Fragment

3.11 Both posterior screws inserted into the proximal articular screw holes of olecranon plate will be of same type.

3.12 For the proximal articular screw holes there are two test groups:

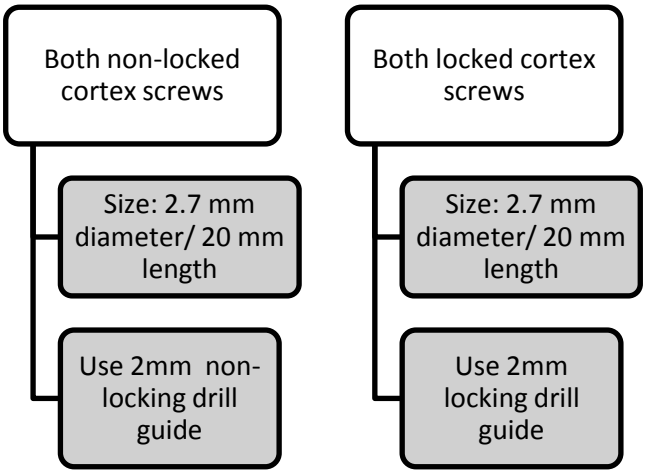

Figure 11: Two Test Groups for Proximal Articular Screw Holes are Shown. Size of Screw and Size of Drill Guide is also Given

3.13 For both test groups a **2mm diameter drill bit** is used to make holes for the screws.

APPENDIX B

NEED REQUIREMENTS AND CHECKLIST TO PERFORM TESTING

All the design requirements were listed in sheet and the status was regularly updated. Below is the table that shows all the design requirements.

Design Requirements	
Fixture and Inventory	
1	Main Fixture/Frame for elbow testing
2	Other components (screws, nuts) for frame
3	Pipe fixture for proximal end
4	Debur the tines
5	Pipe fixture for distal end
6	Making different weight lead balls bags
Document Procedure	
7	Potting procedure for the specimen (Distal)
8	Potting procedure for the specimen (Proximal)
9	Dissection and Suturing procedure
10	Fracture procedure for the study
11	Checklist for all these procedure (combined)
12	DXA scanning of all the specimen (One single day)/ proper protocol
Calculations and coding	
13	MATLAB code for Reaction force calculations
14	MATLAB code for analysis of data
15	Update the weight and size sheet of specimen
16	Failure analysis of pipe and frame
17	Breakdown of forearm length and weight
18	Insert the lead bags in a proper way to increase the weight (5,10...)
19	Calculating COM and length of the specimen through anthropometric data
20	Understanding the working of Optotrek
21	Size of the plate on the shaft of ulna
22	Effect of specimen potting on overall weight?
Before And After Pilot Test	
23	Lab-view code
24	Weight to be used?
25	Cycles to run for each weight?
26	Total time to complete one specimen?
27	ROM should be discrete or continuous?
28	Setting the angular velocity
29	Requirement of instruement and workforce for the elbow testing
30	Alignment of islet on the top and bottom plate

31	Pilot-1 without plate
32	Pilot-2 with plate
33	Minimum and maximum angular displacement
34	Change the potting material to cement (Bondo previously)
35	Scratch the pilot one bondo with sandpaper
36	Timeline document for the testing of the elbow specimen
37	What type of study design should be used for the experiment
Other	
38	Muscle load limits for triceps and brachialis
39	Orientation of the ulna and radius during testing
40	Writing paper and thesis based on the progress made in lab
41	Analysis of quasistatic data and continuous data, comparison as well
42	Landmark and excursion data analysis
43	Knots must be as near as possible to the tendon sutures
44	Use bondo for potting
45	Fragment marker frame
46	Need to order Smith and nephew tray

Checklist developed post validation study for biomechanical testing of olecranon fracture fixation with olecranon plates

Steps
I. Cadaver Preparation
A. DXA scanning of the specimen for density estimation
i) Save the DEXA image and take a print out, keep in file
B. Dissection, suturing and divots
i) Identifying muscle tendons (Triceps and Brachialis)
ii) Suture all three muscle and put the **knots** as near as possible to the suture
iii) Putting divots on a) Epincondyles b) Styloids
iv) Put divots on humeral shaft (sketch a line and insert a wood screw)
TAKE PHOTO
C. Resection and Orientation
i) Verify the styloid divots before resection(ensure the divoted points are most lateral and medial)
ii) Resect the humerus, more than half of the shaft from the distal end or 12 cm
TAKE PHOTO
iii) Resect the ulna-radius 18 cm from the olecranon
TAKE PHOTO
D. Potting
i) Keep ulna & radius in natural posture and put a wood screw at distal end along the shaft (ensure woodscrew does not contact PVC during the potting)
TAKE PHOTO
ii) posterior part of humerus should make contact with the wall of PVC during potting (to ensure proper line of action and avoiding rubbing of tendons on the PVC)
ii) Put the drab/dressing around the tendons and soft tissue
iii) Use appropriate potting mixture/cement
II. Fracture creation
Specimen Thawing Date & Time:
Instrumentation Day & Time:
Test Day & Time:
A. Fracture procedure using fracture protocol doc
I) Be prepare with fracture procedure document
ii) Assemble all the surgical tools and implant components (Plate & screws) before starting this procedure
ii) Use Smith & Nephew tray
iii) Make 3 divots on the fracture line
iii) Make fracture using C-arm and save images
iv) Insert the K-wires into the fragment location for attaching fragment marker frame
v) Reduction procedure
vi) Application of plating technique
vii) Use C-arm and take post images

III. Pre-test day preparation
A. Fixture set-up
**Make a list of hardware and components needed for the test = Cable clamps, crimping tool, screw drivers, extension cords etc.
i) Make an oblique cut to the end of the steel cable and insert it into the hook and crimp it
ii) Verify the length of the steel cable= 8 feet for each speciman
iii) Divot the styloid points through drill bit and mark it with surgical marker
iv) Insert vaseline before inserting the distal or proximal fixture into the bone
v) Verify the length of the distal fixture and bone to be 34 cm **(if not adjust with the other holes in the fixture)**
vi) Insert vaseline into the humerus fixture
vii) Insert the humerus into the fixture and rotate to correct the alignment
viii) Verify the alignment with "level device", Epicondyles parallel to the scale
ix) Lock the humerus with a small wood screw at the third hole on the ROB fixture
x) Put vaseline in the proximal part of the fixture
xi) Orient the distal fixture in line with the bone by rotating the fixture
xii) Attach the 1.5 lb lost muscle mass at 11 cm from proximal
xiii) Lock the fixture with a small wood screw
xiv) Triceps Divoting: Divot the proximal most hole of the plate
xv) Brachialis divot: Divot the solid region (where the tendons enter bone)
xvi) Make knots for the hook of brachilais cable
xvii) Insert screw and drill bit to insert marker frame of ulna
xviii) Use 7/32nd drill bit for marker attachment in radius
IV) Testing Day
A) Arrange the Specimen into the Main Frame & Lab View initial Set Up
i) Rigid body marker attachment, 6D architect to create a new .rig file (_fragXXX and _foreXXX); hot glue the marker buckle
ii) Loads to preposition the arm?
Install the specimen on the frame and take photo
Brach muscle line looping (ensure arm is in full extension)
Multiple obersver to confirm the EL-EM line to be horizontal and optimize for elbow to have a close-to-plane movement within the ROM
Dumbell bar should be in line with humerus
Eyelet positioning and screw tightening
B. Digitization and CoR
iii) NDI: Digitize YY and obtain its coordinates w.r.t. global, ulna & fragment frame;
iv) performed LM digitization and multiple CoR trials in LV (minimum 3) for which the angles computed seemed satisfactory

v) Insert the marker frame on to the two k wire pre drilled into the fragment
vi) Insert the marker frame of ulna
vii) Take pre-setup photo of entire construct
B) NDI, LAB VIEW & Elbow controller setup
i) Open NDI first principles and add files Add probe2 Add frag2 Add fore2 Add _upper
ii) Verify the working of the markers and close NDI first principles
iii) Open LV front panel and Run the program
iv) Fill the test set-up : Specimen Name: xxxxxxxR/L Condition: Weight-cycles-plate type-screw type
v) Select output directory> Make folder for each specimen with ID (L/R arm)> Current folder
vi) Initialize camera as well as run the backend LV
C) Digitization and CoR
i) Origin, X+, XY+ Click apply coordinate changes
ii) Digitize: Epicondyle points Triceps and brachialis eyelets Sup. Humeral shaft point Inf. Humeral shaft point (Please look at the procedure presentation)
iii) Digitize the gap points (Please look at the procedure presentation)
iv) Digitize the Brachialis and Triceps tendon
v) Digitize the Styloid points
vi) NDI: Digitize YY and obtain its coordinates w.r.t. global, ulna & fragment frame;
vii) Perform COR and get the values
D) Proceed to the set up
i) Verfify the test set up Motor 2: Triceps, Max limit: 450N Mult. Window =1 P-gain: 0.5
ii) Motor 7: Brachialis, Max Limit: 200N Mult. Window =1 P-gain: 0.5
iii) Angle control= 0.025
iv) Verify the Motor Matrix Motor 2 = 1 Motor 7 = -1
v) ¨Bring motor 2 and 7 to max position

vi) ¨Tie hook in motor 7 (Brachialis)
vii) ¨Hook the steel cable into the actuator
viii) Put both the motors into force control (5N)
ix) ¨Check the cable is in tension
x) Change both motors to elevation control
xi) Start the test
0 Load condition
i) Fill the test set-up : Specimen Name: xxxxxxxR/L Condition: Weight-cycles-plate type-screw type
ii) Fix the number of cycles in the test setup
iii) Run the test
1.25 Load condition
i) Fill the test set-up : Specimen Name: xxxxxxxR/L Condition: Weight-cycles-plate type-screw type
ii) Fix the number of cycles in the test setup
iii) Run the test
2.5 Load condition
i) Fill the test set-up : Specimen Name: xxxxxxxR/L Condition: Weight-cycles-plate type-screw type
ii) Fix the number of cycles in the test setup
iii) Run the test
3.75 Load condition
i) Fill the test set-up : Specimen Name: xxxxxxxR/L Condition: Weight-cycles-plate type-screw type
ii) Fix the number of cycles in the test setup
iii) Run the test
5 Load condition
i) Fill the test set-up : Specimen Name: xxxxxxxR/L Condition: Weight-cycles-plate type-screw type
ii) Fix the number of cycles in the test setup
iii) Run the test
End Of Experiment